



Article

Impacts of Crop Type and Climate Changes on Agricultural Water Dynamics in Northeast China from 2000 to 2020

Xingyuan Xiao ¹ , Jing Zhang ¹ and Yaqun Liu ^{1,2,*}

¹ College of Geodesy and Geomatics, Shandong University of Science and Technology, Qingdao 266590, China; skd991338@sdust.edu.cn (X.X.); 202183020053@sdust.edu.cn (J.Z.)

² Key Laboratory of Regional Sustainable Development Modeling, Institute of Geographic Sciences and Natural Resources Research, Chinese Academy of Sciences, Beijing 100101, China

* Correspondence: liuyaqun@igsnr.ac.cn

Abstract: Northeast China (NEC) is one of the most important national agricultural production bases, and its agricultural water dynamics are essential for food security and sustainable agricultural development. However, the dynamics of long-term annual crop-specific agricultural water and its crop type and climate impacts remain largely unknown, compromising water-saving practices and water-efficiency agricultural management in this vital area. Thus, this study used multi-source data of the crop type, climate factors, and the digital elevation model (DEM), and multiple digital agriculture technologies of remote sensing (RS), the geographic information system (GIS), the Soil Conservation Service of the United States Department of Agriculture (USDA-SCS) model, the Food and Agriculture Organization of the United Nations Penman–Monteith (FAO P-M) model, and the water supply–demand index (M) to map the annual spatiotemporal distribution of effective precipitation (Pe), crop water requirement (ET_c), irrigation water requirement (IWR), and the supply–demand situation in the NEC from 2000 to 2020. The study further analyzed the impacts of the crop type and climate changes on agricultural water dynamics and revealed the reasons and policy implications for their spatiotemporal heterogeneity. The results indicated that the annual average Pe, ET_c, IWR, and M increased by 1.56%/a, 0.74%/a, 0.42%/a, and 0.83%/a in the NEC, respectively. Crop-specifically, the annual average Pe increased by 1.15%/a, 2.04%/a, and 2.09%/a, ET_c decreased by 0.46%/a, 0.79%/a, and 0.89%/a, IWR decreased by 1.03%/a, 1.32%/a, and 3.42%/a, and M increased by 1.48%/a, 2.67%/a, and 2.87%/a for maize, rice, and soybean, respectively. Although the ET_c and IWR for all crops decreased, regional averages still increased due to the expansion of water-intensive maize and rice. The crop type and climate changes jointly influenced agricultural water dynamics. Crop type transfer contributed 39.28% and 41.25% of the total IWR increase, and the remaining 60.72% and 58.75% were caused by cropland expansion in the NEC from 2000 to 2010 and 2010 to 2020, respectively. ET_c and IWR increased with increasing temperature and solar radiation, and increasing precipitation led to decreasing IWR in the NEC. The adjustment of crop planting structure and the implementation of water-saving practices need to comprehensively consider the spatiotemporally heterogeneous impacts of crop and climate changes on agricultural water dynamics. The findings of this study can aid RS-GIS-based agricultural water simulations and applications and support the scientific basis for agricultural water management and sustainable agricultural development.

Keywords: agricultural water use; irrigation water requirement; crop planting structure change; climatic change; spatiotemporally heterogeneous impacts; water-efficient management



Citation: Xiao, X.; Zhang, J.; Liu, Y. Impacts of Crop Type and Climate Changes on Agricultural Water Dynamics in Northeast China from 2000 to 2020. *Remote Sens.* **2024**, *16*, 1007. <https://doi.org/10.3390/rs16061007>

Academic Editor: Annamaria Castrignanò

Received: 10 January 2024

Revised: 6 March 2024

Accepted: 11 March 2024

Published: 13 March 2024



Copyright: © 2024 by the authors. Licensee MDPI, Basel, Switzerland. This article is an open access article distributed under the terms and conditions of the Creative Commons Attribution (CC BY) license (<https://creativecommons.org/licenses/by/4.0/>).

1. Introduction

Water is one of the most important material resources for the development of human society, and it is indispensable for any production process [1]. With rapid socio-economic development and environmental deterioration over the past century, water scarcity has become a thorny problem [2]. More than 40 countries (about 40% of the world's population)

face the challenge of water scarcity, which seriously limits their sustainable economic development [3,4]. There are many reasons for water scarcity; specifically, global population growth, climate change, excessive industrial production, rapid urbanization, and the expansion of agricultural land have all led to an increased demand for water [5–7]. Agriculture accounts for 70% of the world’s water resources [8,9]. Therefore, it is critical to understand the water supply and demand in the agricultural sector and explore rational water allocation to help to maintain sustainable agricultural development.

As the world’s leading agricultural nation, the crop irrigation water requirement in China constitutes over 90% of the total agricultural water requirement [10]. The agricultural irrigation requirement is the key to growing crops and sustainable food production and security [11]. As a result, the crop irrigation water requirement has received significant attention [12,13]. The increase in the irrigation water requirement has resulted in an increasing trend in crop yield [14]. Only 20% of the world’s irrigated land had grown over 40% of the grain production yield, and irrigated land yields roughly 2.5 times the grain production compared to non-irrigated land [15]. Approximately three-quarters of the grain production was cultivated in irrigated farmland [16,17]. In the late 1960s, our country made great efforts to build irrigation infrastructure on farmland and this led to crop yield increasing rapidly [10].

The crop irrigation water requirement is expressed as the difference between the crop water requirement and the effective precipitation [18,19]. Methods for calculating the irrigation water requirement include field observation, non-spatial crop models, and the spatial crop method (Table 1). The first method obtains a mass conservation function for calculating the crop irrigation water requirement by considering the relevant parameters [20,21]. The second method uses point data of reference evapotranspiration and crop coefficient values from the available literature, with over 100 different crop models available [22]. The most frequently utilized models include CROPWAT, AquaCrop, and PolyCrop [23]. CROPWAT is a model developed by the Food and Agriculture Organization of the United Nations (FAO) in 1991 to calculate crop water requirements and it plays a significant role in crop water requirement estimation for different regions and crop types [24]. AquaCrop has the advantages of simple input parameters, a simple interface, and stable simulation results [25]. PolyCrop can calculate variations in the water requirement for a crop cultivation system based on crop type changes and growth seasons [26]. However, these models cannot address irrigation water changes caused by the crop type and spatiotemporal differences. The third method can predict the spatial distribution of the relevant data, which can directly reflect spatiotemporal changes and help to reveal spatial phenomena and laws [27,28]. However, considering the lack of a spatial crop model, conducting long-term annual crop-specific studies has great significance for gaining insight into the water dynamics of major crops.

Table 1. Advantages and disadvantages of methods for estimating crop irrigation water requirements.

Method Type	Advantages	Disadvantages	References
Field observation	Obtain more accurate agricultural water data at a finer temporal resolution (e.g., second, minute, hour)	Time-consuming, labor-intensive, and expensive to conduct large-area experiments	[29,30]
Non-spatial crop model	Simulate agricultural water use for different crops at different growth periods at the point scale	Difficult to reveal fine-resolution spatial characteristics	[31,32]
Spatial crop model	Simulate spatiotemporal distribution of agricultural water use at a finer raster scale	Currently lacking a long-term annual crop-type-specific study	[33,34]

As one of the most crucial grain production bases in China, the agricultural irrigation water requirement accounts for 78% of the total water in Northeast China (NEC) [35,36].

The crop planting structure has been largely adjusted in recent years, especially having rapidly expanded the area of the water-intensive crops but reduced the water-saving soybean crops [37]. This has led to an increase in the regional crop irrigation water requirement [38,39]. In addition, climate changes have an impact on the crop irrigation water requirement [40–42]. However, previous studies have mainly focused on the spatiotemporal changes in the crop water requirement for a specific crop type and analyzed the effects of climate changes or crop type changes on irrigation water requirement, rather than discussing these on a raster scale [43–46]. In addition, there are few research studies on long-term changes, annually analyzing spatiotemporal changes in the crop water requirement [47–49]. This study used multi-source remote-sensing (RS) data and digital agriculture technologies to map the annual crop-specific spatiotemporal distribution of effective precipitation (P_e), crop water requirement (ET_c), irrigation water requirement (IWR), and water supply–demand index (M), reveal the impacts of the crop type and climate changes on agricultural water dynamics in the NEC from 2000–2020, and discuss the policy recommendations and future research topics for integrated water resource management and sustainable agricultural development.

2. Materials

2.1. Study Area

The NEC ($38^{\circ}52'–53^{\circ}55'N$, $115^{\circ}52'–135^{\circ}09'E$) consists of three provinces of Heilongjiang, Jilin, Liaoning, and the four eastern leagues of the Inner Mongolia Autonomous Region (Chifeng, Tongliao, Xing'an, and Hulunbeier), covering an area of 1.24×10^6 km² (Figure 1a). The region straddles the mesothermal and subfreezing zones from south to north and has a temperate monsoon climate with distinct seasons. It has warm, rainy summers and cold, dry winters. From the southeast to the northwest, the annual precipitation drops from 1000 mm to less than 300 mm, and the transition is from a humid and semi-humid area to semi-arid area. The NEC has fertile black soil, accounting for approximately 12% of the total area of the world's total black soil area, which makes the NEC one of the main grain-producing areas in China, representing a quarter of the country's total food production. The main food crops are mainly distributed in the central and southern areas of maize, the eastern area of rice, and the northern and northwestern areas of soybean, respectively (Figure 1b).

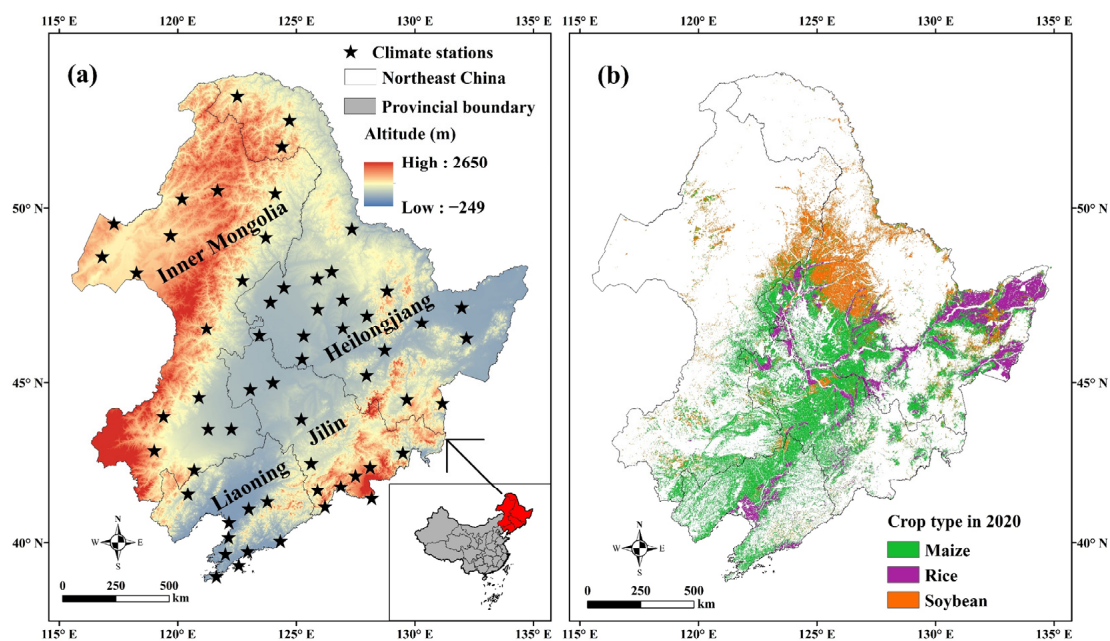


Figure 1. Geographical location, climate stations (a), and crop type distribution (b) in the NEC.

2.2. Data Sources

The multi-source data used in this study included climate factors, crop type RS products, the digital elevation model (DEM), and the administrative boundary.

Climate factors included daily field observations of temperature (maximum, minimum, and average), precipitation, wind speed, relative humidity, atmospheric pressure, and sunshine hours in the NEC from 2000 to 2020, which were from 60 climate stations of the National Meteorological Science Data Center (<https://data.cma.cn/>, accessed on 25 July 2023). We further spatially interpolated the field observations into 500 m spatial resolution daily raster data using the thin-plate spline method that introduced DEM as a covariate in the ANUSPLIN version 4.3 software [50]. The monthly averages of these climate factors in Heilongjiang, Jilin, Liaoning, and Inner Mongolia are shown in Table 2.

Table 2. Monthly climate factors for the four areas in the NEC.

Month	Area	Climate Factors							
		Maximum Temperature (°C)	Minimum Temperature (°C)	Average Temperature (°C)	Precipitation (mm)	Wind Speed (m/s)	Relative Humidity (%)	Atmospheric Pressure (Pa)	Sunshine Hours (h)
January	Heilongjiang	−13.57	−25.45	−20.09	4.99	2.19	69.18	993.87	171.25
	Jilin	−7.97	−20.06	−14.60	6.96	2.01	64.94	976.46	177.41
	Liaoning	−2.03	−11.46	−7.21	5.40	2.76	56.12	1017.76	196.40
	Inner Mongolia	−12.16	−23.81	−18.70	2.41	2.40	58.97	966.54	196.40
February	Heilongjiang	−8.33	−22.08	−15.63	5.05	2.44	64.36	991.40	198.53
	Jilin	−3.11	−15.88	−9.85	12.05	2.35	58.18	974.38	188.84
	Liaoning	1.52	−7.86	−3.54	10.49	2.92	54.25	1015.39	193.63
	Inner Mongolia	−7.02	−20.51	−14.42	2.60	2.63	54.90	964.08	218.92
March	Heilongjiang	1.32	−11.54	−5.16	11.19	2.95	59.31	986.48	244.55
	Jilin	4.88	−7.14	−1.39	18.75	2.79	58.96	969.96	221.71
	Liaoning	8.22	−1.34	3.10	13.76	3.28	53.03	1010.21	242.42
	Inner Mongolia	2.50	−11.40	−4.70	5.60	3.08	50.25	959.89	270.01
April	Heilongjiang	12.00	−0.83	5.58	23.52	3.25	52.18	982.10	232.49
	Jilin	14.34	1.32	7.64	36.21	2.99	49.89	966.06	216.37
	Liaoning	15.93	5.92	10.67	41.13	3.48	53.01	1004.48	242.30
	Inner Mongolia	13.17	−0.85	6.16	14.59	3.44	41.43	955.45	265.33
May	Heilongjiang	20.26	7.04	13.72	54.52	3.08	56.55	978.81	243.01
	Jilin	21.80	8.56	14.96	69.68	2.79	56.98	963.02	236.58
	Liaoning	22.50	12.46	17.22	62.06	3.11	59.44	1000.48	266.99
	Inner Mongolia	21.51	7.07	14.44	33.51	3.29	43.77	951.83	275.39
June	Heilongjiang	25.62	13.50	19.49	92.08	2.51	67.75	977.81	243.81
	Jilin	25.85	14.23	19.66	95.09	2.24	68.18	961.38	221.58
	Liaoning	26.10	17.48	21.47	86.03	2.67	71.68	997.34	225.16
	Inner Mongolia	26.75	13.45	20.16	69.11	2.58	56.46	950.63	267.59
July	Heilongjiang	27.27	17.02	21.92	138.76	2.27	77.46	977.12	229.42
	Jilin	27.81	18.11	22.51	156.72	2.02	76.61	960.83	206.85
	Liaoning	28.43	21.18	24.48	142.83	2.52	78.98	996.18	200.08
	Inner Mongolia	28.49	16.78	22.46	98.14	2.34	66.67	949.94	263.09
August	Heilongjiang	25.62	15.14	20.00	114.65	2.15	78.95	980.47	224.13
	Jilin	26.97	16.95	21.38	148.62	1.84	78.20	963.81	210.89
	Liaoning	28.54	20.79	24.29	179.12	2.36	79.00	999.05	218.12
	Inner Mongolia	26.65	14.52	20.25	77.26	2.24	67.81	953.60	259.81
September	Heilongjiang	20.45	7.75	13.66	57.72	2.36	71.27	985.42	224.84
	Jilin	22.35	9.74	15.37	59.36	1.90	72.20	969.31	217.58
	Liaoning	24.86	15.16	19.61	51.74	2.42	70.77	1005.64	233.24
	Inner Mongolia	21.28	7.16	13.74	33.42	2.43	60.30	958.43	247.49
October	Heilongjiang	10.73	−1.31	4.31	23.80	2.67	62.39	988.54	197.94
	Jilin	14.26	1.33	7.19	35.80	2.25	62.29	972.87	205.35
	Liaoning	17.53	7.45	12.14	42.84	2.74	73.14	1011.76	215.01
	Inner Mongolia	11.54	−1.83	4.28	13.93	2.67	53.80	961.80	229.27
November	Heilongjiang	−2.43	−13.07	−8.15	13.10	2.53	66.35	990.89	162.43
	Jilin	2.78	−7.73	−2.91	26.15	2.26	64.93	974.56	160.53
	Liaoning	8.02	−0.92	3.21	26.25	2.97	60.20	1014.22	177.53
	Inner Mongolia	−1.26	−12.91	−7.69	6.57	2.53	58.96	963.53	185.90
December	Heilongjiang	−12.53	−23.06	−18.23	8.08	2.49	69.96	992.83	151.10
	Jilin	−6.37	−17.24	−12.24	11.22	2.12	66.11	975.93	178.28
	Liaoning	0.02	−8.78	4.74	9.65	2.81	58.34	1017.14	178.28
	Inner Mongolia	−10.82	−21.55	−16.76	3.93	2.44	61.56	965.56	174.75

The crop type RS products were the 500 m spatial resolution annual distributions of maize, rice, and soybean in the NEC from 2000 to 2020, which were provided by Liu and Wang [37]. The crop type data were obtained using 111-dimensional MOD09A1 features, recursive feature elimination, and random forest algorithms on the Google Earth Engine (GEE) platform, with the sample-based classification accuracies of 84.73–86.93% and a statistics-based R^2 of 0.81–0.95.

DEM data were sourced from the Resource and Environmental Science and Data Center of the Chinese Academy of Sciences (<https://www.resdc.cn/>, accessed on 25 July 2023), with a spatial resolution of 500 m.

National and provincial administrative boundary data were the 2015 multi-level national vector map from the Resource and Environmental Science and Data Center of the Chinese Academy of Sciences (<https://www.resdc.cn/>, accessed on 25 July 2023).

3. Methods

In this study, based on multi-source data of daily climate data, DEM, and crop type RS data, we first used the Soil Conservation Service of the United States Department of Agriculture (USDA-SCS) model to calculate P_e and used the RS-based FAO Penman–Monteith (P-M) model to estimate ET_c in the NEC from 2000 to 2020 (Figure 2). Second, we used the FAO IWR formula to calculate the IWR and applied the water supply–demand index (M) to evaluate the agricultural water supply–demand situation. Third, we adopted transfer matrix-based statistics to estimate the IWR change and its contribution rate caused by different crop type transfers and used a gradient boxplot to reveal the impact of climate change on the ET_c and IWR.

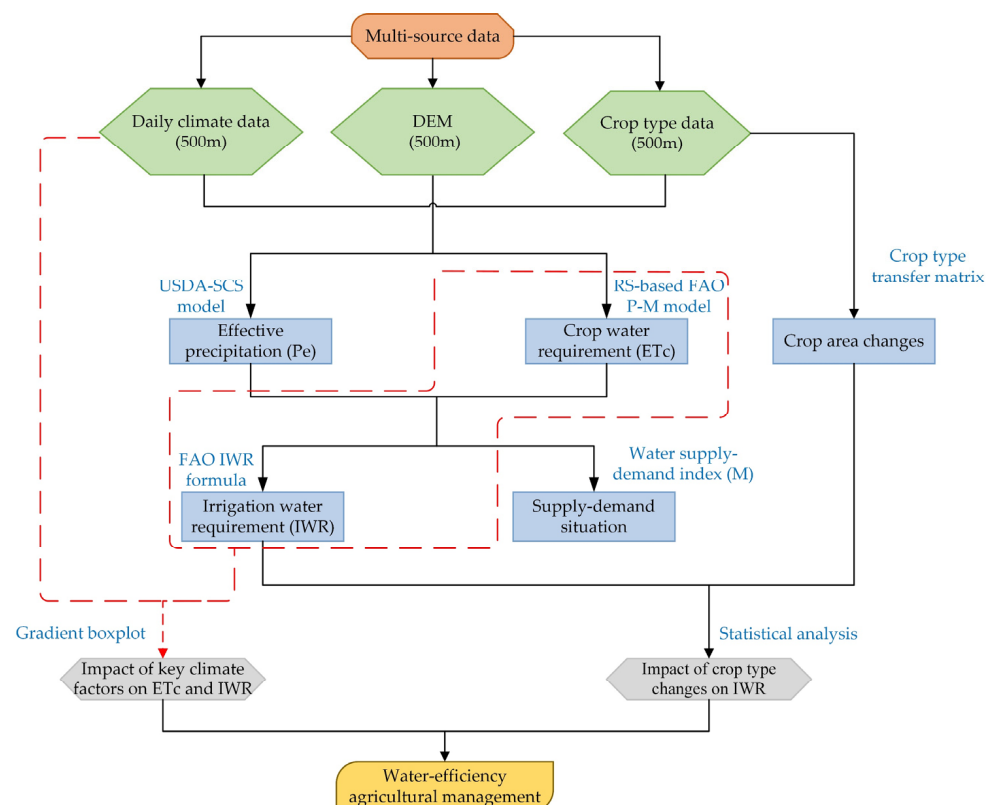


Figure 2. Research framework for crop water requirement.

3.1. Calculation of Effective Precipitation

Effective precipitation is the amount of precipitation that can be effectively used, excluding surface runoff and seepage below the crop root zone [23]. There are more effective precipitation influencing factors, such as crop type and physiological characteristics, soil

texture, and climate changes. This study used the USDA-SCS model to calculate the daily effective precipitation (Pe) during the crop growth period [51–53]. The formula for Pe was as follows:

$$Pe = \begin{cases} P \times (4.17 - 0.2)/4.17 & P < 8.3 \\ 4.17 + 0.1 \times P & P \geq 8.3 \end{cases} \quad (1)$$

where Pe is the daily effective precipitation (mm), and P is the daily precipitation (mm).

3.2. Calculation of Crop Water Requirement

This study used daily climate raster data and the FAO P-M model to calculate reference crop evapotranspiration (ET_o) and the crop water requirement (ET_c) [54], by adopting the crop type RS products to obtain the crop-specific spatial distribution of key crop parameters. Notably, the parameters for a certain crop in this study were the same in space. The formula for ET_o was as follows:

$$ET_o = \frac{0.408 \times \Delta(R_n - G) + \gamma \times \frac{900}{T+273} \times u_2(e_s - e_a)}{\Delta + \gamma(1 + 0.34 \times u_2)} \quad (2)$$

where ET_o is the reference crop evapotranspiration (mm/d); Δ is the slope of the saturated water vapor pressure–temperature curve (KPa/°C); R_n is the net crop canopy surface radiation (MJ/(m²·d)); G is the soil heat flux (MJ/(m²·d)), when calculating with daily climate data, $G = 0$; γ is the psychrometric constant (KPa/°C); T is the average temperature at 2 m (°C); u_2 is the average wind speed at 2 m (m/s); e_s is the saturated water vapor pressure (KPa); e_a is the actual vapor pressure (KPa); $e_s - e_a$ is the saturation pressure deficit (KPa).

The crop water requirement (ET_c) is determined by crop coefficients and the reference crop evapotranspiration. The formula for ET_c was as follows:

$$ET_{c,i} = K_{c,i} \times ET_o \quad (3)$$

where i is the crop type; $ET_{c,i}$ is the crop water requirement (mm); $K_{c,i}$ is the crop coefficient during various growth periods, which is calculated using the single crop coefficient method; K_c is categorized according to the growth periods of the crop into $K_{c,ini}$ (during the initial and rapid growth period), $K_{c,mid}$ (during the mid-growth period), and $K_{c,end}$ (during the final growth period). The K_c values for the three crops were based on the crop fertility situation (Table 3) and relevant experimental results [55].

Table 3. The growth period and K_c coefficients of three crops in the NEC.

Growth Period and K_c	Maize	Rice	Soybean
Sowing Date	27 April	15 May	30 April
End Date	20 September	25 September	25 September
Growth Period (d)	147	134	149
$K_{c,ini}$	0.49	1.15	0.32
$K_{c,mid}$	1.06	1.25	0.73
$K_{c,end}$	0.58	1.05	0.32

Note: K_c is the average values of the three crops at different growth periods.

3.3. Calculation of Irrigation Water Requirement

The crop irrigation water requirement (IWR) is the difference between the crop water requirement and the effective precipitation [56]. The formula for IWR was as follows:

$$IWR_i = \begin{cases} ET_{c,i} - Pe_i & ET_{c,i} > Pe_i \\ 0 & ET_{c,i} \leq Pe_i \end{cases} \quad (4)$$

where IWR_i is the irrigation water requirement of crop i during the growth period (mm); $ET_{c,i}$ is the crop water requirement of crop i during the growth period (mm); Pe_i is the effective precipitation of crop i during the growth period (mm).

3.4. Calculation of Water Supply–Demand Index

The water supply–demand index reflects the relationship between the effective supply and demand of regional agricultural available water resources [46]. The formula for M was as follows:

$$M_i = \frac{W_i}{D_i} \quad (5)$$

where M_i is the water supply–demand index for crop i ; W_i is the effective water supply for crop i during the growth period, which is the effective precipitation (Pe); D_i is the crop water requirement for crop i during the growth period (ET_c). Normally, the value of M ranges from 0 to 1. The larger the M value, the better the matching degree, whereas the smaller the M value, the poorer the matching degree. When $M \geq 1$, the crop effective precipitation has met the irrigation water requirement.

3.5. Linear Regression Trend Analysis

This study used linear regression to analyze the trends of Pe , ET_c , IWR , and M for different crops from 2000 to 2020 in the NEC. The slope in the regression equation represents the inter-annual variability and is calculated using the least squares method. The formula for *slope* was as follows:

$$slope = \frac{n \times \sum_{t=1}^n t \times W_t - (\sum_{t=1}^n t)(\sum_{t=1}^n W_t)}{n \times \sum_{t=1}^n t^2 - (\sum_{t=1}^n t)^2} \quad (6)$$

$$slope\% = slope \times \frac{n}{\sum_{t=1}^n W_t} \times 100 \quad (7)$$

where *slope* is the inter-annual trend, n is the number of years; W_t is the value of this index (Pe , ET_c , IWR , M) in year t ; a positive *slope* indicates an increasing trend and a negative *slope* indicates a decreasing trend; *slope%* is the ratio of *slope* to the multi-year average W , which aims to calculate the magnitude of change in the multi-year average of W .

4. Results

4.1. Annual Spatial Distribution and Temporal Changes in Pe

The average of Pe in the NEC from 2000 to 2020 showed a slowly increasing trend (Figure 3). The average Pe value reached its highest value of 239.39 mm in 2019, while it reached its lowest value of 153.13 mm in 2007. The slope of Pe in 2000–2020 was 2.99 mm/a and the slope% was 1.56%/a (Table 4). The average Pe for maize, rice, and soybean showed an upward trend (Figure 4a). The average Pe for maize reached its highest value of 242.72 mm in 2005, while it reached its lowest value of 158.62 mm in 2000. The average Pe for rice reached its highest value of 266.88 mm in 2019, while it reached its lowest value of 144.83 mm in 2007. The average Pe for soybean reached its highest value of 252.33 mm in 2019, while it reached its lowest value of 131.11 mm in 2007. The multi-year average Pe for the three crops was 195.52 mm, 180.68 mm, and 193.28 mm, respectively. The slope of Pe from 2000 to 2020 for maize, rice, and soybean was 2.24 mm/a, 3.69 mm/a, and 4.04 mm/a, respectively, and the slope% was 1.15%/a, 2.04%/a, and 2.09%/a, respectively (Table 4).

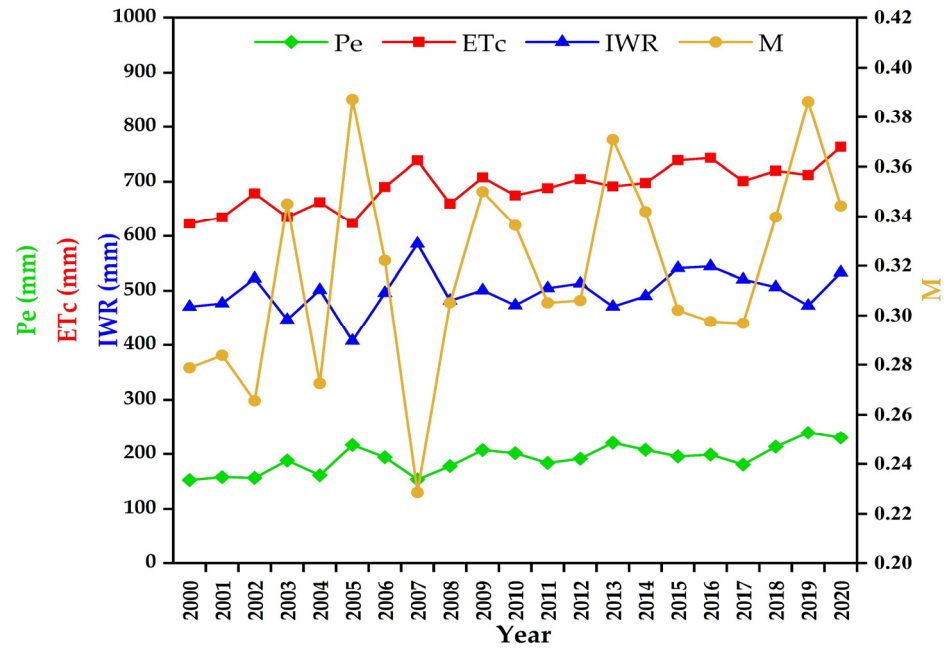


Figure 3. The annual average Pe, ET_c , IWR, and M values in the NEC from 2000 to 2020.

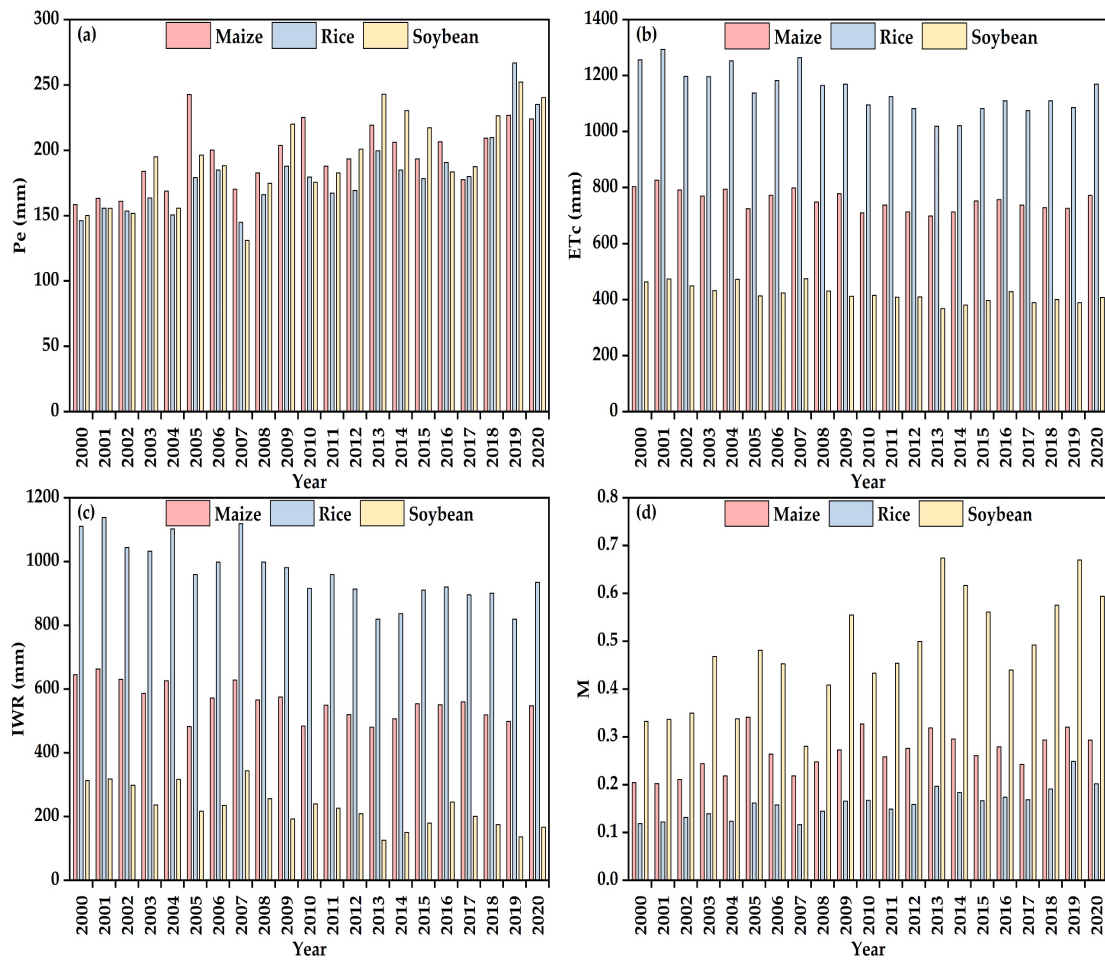


Figure 4. The annual average Pe (a), ET_c (b), IWR (c), and M values (d) for different crop types in the NEC from 2000 to 2020.

Table 4. Slope and slope% of Pe, ET_c, IWR, and M for different crops in the NEC from 2000 to 2020.

Crop Type	Pe		ET _c		IWR		M	
	Slope (mm/a)	Slope% (/a)	Slope (mm/a)	Slope% (/a)	Slope (mm/a)	Slope% (/a)	Slope (/a)	Slope% (/a)
Maize	2.24	1.15	−3.50	−0.46	−5.77	−1.03	0.004	1.48
Rice	3.69	2.04	−9.09	−0.79	−12.73	−1.32	0.004	2.67
Soybean	4.04	2.09	−3.76	−0.89	−7.80	−3.42	0.01	2.87

The average of Pe for maize was the highest in Liaoning at 207.28 mm and the lowest in Inner Mongolia at 155.72 mm (Table 5). The average of Pe for rice was the highest in Liaoning at 184.10 mm and the lowest in Inner Mongolia at 151.55 mm. The average of Pe for soybean was the highest in Heilongjiang at 206.79 mm and the lowest in Liaoning at 165.45 mm. The standard deviation of Pe for maize was the highest in Jilin at 40.08 mm and the lowest in Liaoning at 17.98 mm. The standard deviation of Pe for rice was the highest in Heilongjiang at 56.57 mm and the lowest in Inner Mongolia at 39.45. The standard deviation of Pe for soybean was the highest in Jilin at 37.40 mm and the lowest in Liaoning at 10.81 mm.

Table 5. The average and standard deviation Pe, ET_c, IWR, and M values of different crops for the four areas in the NEC from 2000 to 2020.

Crop Type	Area	Pe (mm)		ET _c (mm)		IWR (mm)		M	
		Average	Standard Deviation	Average	Standard Deviation	Average	Standard Deviation	Average	Standard Deviation
Maize	Heilongjiang	207.25	28.56	729.70	226.83	522.76	254.99	0.29	0.099
	Jinlin	207.28	40.08	749.82	169.89	542.07	276.45	0.28	0.102
	Liaoning	180.56	17.98	773.22	149.37	591.57	251.38	0.24	0.062
	Inner Mongolia	155.72	25.56	825.91	262.58	669.69	149.16	0.19	0.069
Rice	Heilongjiang	182.47	56.57	1142.03	255.98	960.23	183.28	0.164	0.085
	Jinlin	184.10	50.36	1166.39	283.61	981.91	139.70	0.162	0.077
	Liaoning	161.72	41.96	1178.45	250.53	1015.12	129.48	0.14	0.068
	Inner Mongolia	151.55	39.45	1249.20	158.41	1097.31	226.28	0.12	0.043
Soybean	Heilongjiang	206.79	12.83	404.78	55.22	198.02	60.07	0.53	0.06
	Jinlin	174.92	37.40	450.86	49.97	275.94	77.11	0.40	0.12
	Liaoning	165.45	10.81	455.04	34.04	289.59	33.82	0.37	0.03
	Inner Mongolia	174.08	19.72	443.34	57.28	266.43	70.10	0.41	0.08

The Pe had different spatial changes in 2000–2020 in the NEC (Figure 5). The average Pe from west to east showed a trend of first increasing, then decreasing and then increasing in the whole NEC during the past two decades. The maximum standard deviation of Pe was mainly distributed in the eastern area in Heilongjiang, and the minimum standard deviation of Pe was mainly distributed in the southeastern area in Inner Mongolia. Pe in Inner Mongolia generally showed a trend of being low in the central area and high in the northern and southern areas. Heilongjiang was higher in the southeastern area, with a southeast–northwest dividing line and a decreasing trend towards both sides. Jilin showed a trend of gradual decrease from the southeastern to the northwestern area. Liaoning showed a gradual trend of decreasing from the eastern to the western area. The maximum value of Pe was mainly distributed in the southeastern area in the NEC from 2000 to 2011, which moved gradually from the southeastern to the central–eastern area from 2012 to 2020 in the NEC. The minimum value of Pe was mainly distributed in the central and eastern areas in the NEC.

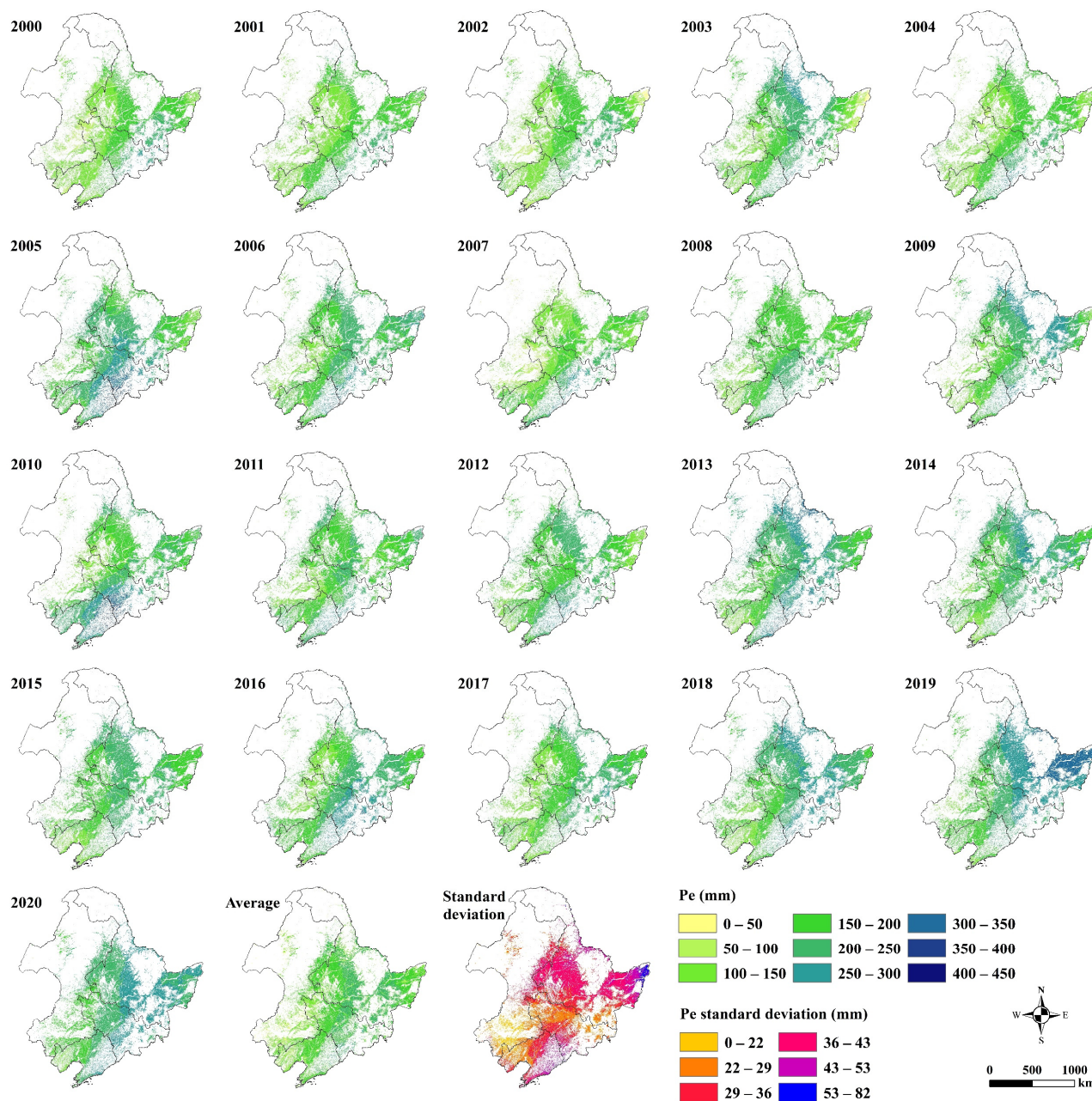


Figure 5. The spatial distribution of annual Pe and their average and standard deviation in the NEC from 2000 to 2020.

4.2. Annual Spatial Distribution and Temporal Changes in ET_c

The average ET_c in the NEC showed a gradual increase from 2000 to 2020 (Figure 3). The average ET_c reached the highest value of 763.27 mm in 2020, while reached the lowest value of 622.93 mm in 2000. The slope of ET_c was 5.09 mm/a and the slope% was 0.74%/a (Table 4). The average of ET_c for maize, rice, and soybean showed a decreasing trend (Figure 4b). The average ET_c for maize reached the highest value of 826.50 mm in 2001, while it reached the lowest value of 699.27 mm in 2013. The average ET_c for rice reached the highest value of 1294.11 mm in 2001, while it reached the lowest value of 1019.20 mm in 2013. The average ET_c for soybean reached the highest value of 474.97 mm in 2007, while it reached the lowest value of 368.42 mm in 2013. The multi-year average ET_c values for the three crops were 755.21 mm, 1147.53 mm, and 421.29 mm, respectively. The slope of ET_c from 2000 to 2020 for maize, rice, and soybean was -3.50 mm/a, -9.09 mm/a,

and -3.76 mm/a, respectively, and the slope% was $-0.46\%/a$, $-0.79\%/a$, and $-0.89\%/a$, respectively (Table 4).

The average of ET_c for maize was the highest in Inner Mongolia at 825.91 mm and the lowest in Heilongjiang at 729.70 mm (Table 5). The average of ET_c for rice was the highest in Inner Mongolia at 1249.20 mm and the lowest in Heilongjiang at 1142.03 mm. The average of ET_c for soybean was the highest in Liaoning at 455.04 mm and the lowest in Heilongjiang at 404.78 mm. The standard deviation of ET_c for maize was the highest in Inner Mongolia at 262.58 mm and the lowest in Liaoning at 149.37. The standard deviation of ET_c for rice was the highest in Jilin at 283.61 mm and the lowest in Inner Mongolia at 158.41 mm. The standard deviation of ET_c for soybean was the highest in Inner Mongolia at 57.28 mm and the lowest in Liaoning at 34.04 mm.

The ET_c had different spatial changes in 2000–2020 in the NEC (Figure 6). The average ET_c from north to south and from west to east showed a gradual trend of increasing in the whole NEC during the past two decades. The maximum standard deviation of ET_c was mainly distributed in the eastern area in Heilongjiang, and the minimum standard deviation of ET_c was mainly distributed in the southwestern area in Liaoning. The ET_c of Inner Mongolia generally showed a trend of being higher in the southern area and lower in the northern area. Heilongjiang expanded from the center to the surroundings, which showed a trend of being lower in the central area and higher in the surroundings. Jilin and Liaoning had basically the same trend, both of which showed a decreasing trend from the central area to the surroundings. The maximum value of ET_c was mainly in the southern and eastern areas from 2000 to 2001 in the NEC. Since 2002, the maximum value of ET_c has gradually moved from the southern to the northern area until the south–central area in the NEC. The eastern area of the NEC has remained one of the major distribution areas for the ET_c maximum. The spatial distribution of the minimum value of ET_c was basically unchanged from 2000 to 2020, it was still mainly found in the central area of Heilongjiang and eastern–central area of Inner Mongolia.

4.3. Annual Spatial Distribution and Temporal Changes in IWR

The average IWR in the NEC showed a gradual increase from 2000 to 2020 (Figure 3). The average IWR reached the highest value of 706.71 mm in 2001, while it reached the lowest value of 475.08 mm in 2013. The slope of IWR was 2.08 mm/a and the slope% was 0.42%/a (Table 4). The average of IWR for maize, rice, and soybean showed a decreasing trend (Figure 4c). Crop types varied in the irrigation water requirement. The average IWR for maize reached the highest value of 663.19 mm in 2001, while it reached the lowest value of 480.01 mm in 2013. The average IWR for rice reached the highest value of 1138.41 mm in 2001, while it reached the lowest value of 819.55 mm in 2013. The average IWR for soybean reached the highest value of 343.87 mm in 2007, while it reached the lowest value of 125.68 mm in 2013. The multi-year average IWR for maize, rice, and soybean was 559.51 mm, 967.12 mm, and 228.00 mm, respectively. The slope of IWR from 2000 to 2020 for maize, rice, and soybean was -5.77 mm/a, -12.73 mm/a, and -7.80 mm/a, and the slope% was $-1.03\%/a$, $-1.32\%/a$, and $-3.42\%/a$, respectively (Table 4).

The average of IWR for maize was the highest in Inner Mongolia at 669.69 mm and the lowest in Heilongjiang at 522.76 mm (Table 5). The average of IWR for rice was the highest in Inner Mongolia at 1097.31 mm and the lowest in Heilongjiang at 960.23 mm. The average of IWR for soybean was the highest in Liaoning at 289.59 mm and the lowest in Heilongjiang at 198.02 mm. The standard deviation of IWR for maize was the highest in 276.45 mm and the lowest in Inner Mongolia at 149.16 mm. The standard deviation of IWR for rice was the highest in Inner Mongolia at 226.28 mm and the lowest in Liaoning at 129.48 mm. The standard deviation of IWR for soybean was the highest in Jinlin at 77.11 mm and the lowest in Liaoning at 33.82 mm.

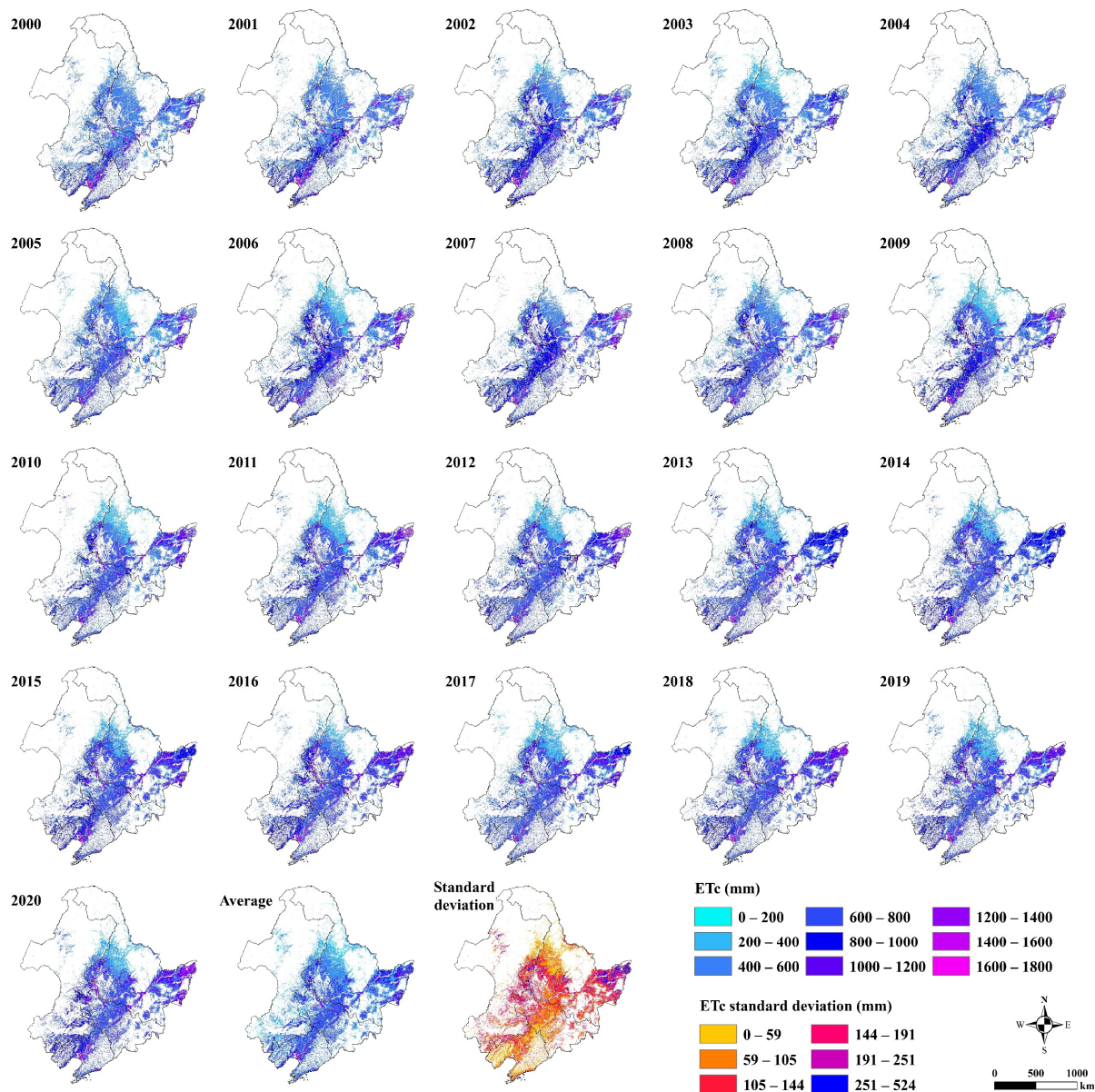


Figure 6. The spatial distribution of annual ET_c and their average and standard deviation in the NEC from 2000 to 2020.

The IWR had different spatial changes in 2000–2020 in the NEC (Figure 7). The average IWR showed a gradually increasing trend from north to south in the whole NEC during the past two decades. The maximum standard deviation of IWR was mainly distributed in the eastern area in Heilongjiang, and the minimum was mainly distributed in the northern area in Heilongjiang. Inner Mongolia showed an increasing trend from the northern to the southern area. Heilongjiang expanded from the center to the surroundings, which showed a trend of being lower in the central area and higher in the surroundings. Jilin showed a trend of gradual decrease from the northeastern to the southwestern area. Liaoning showed a decreasing trend from the center to the surroundings. The maximum value of IWR was mainly in the south–central and eastern areas in the NEC from 2000 to 2001. Since 2002, the maximum value of IWR has gradually moved from Liaoning to the central area in the NEC. The eastern area of the NEC has remained one of the major distribution areas for IWR maximum. The spatial distribution of the minimum value of IWR was relatively unchanged from 2000 to 2020; it was still mainly concentrated in the central area of Heilongjiang and eastern–central area of Inner Mongolia.

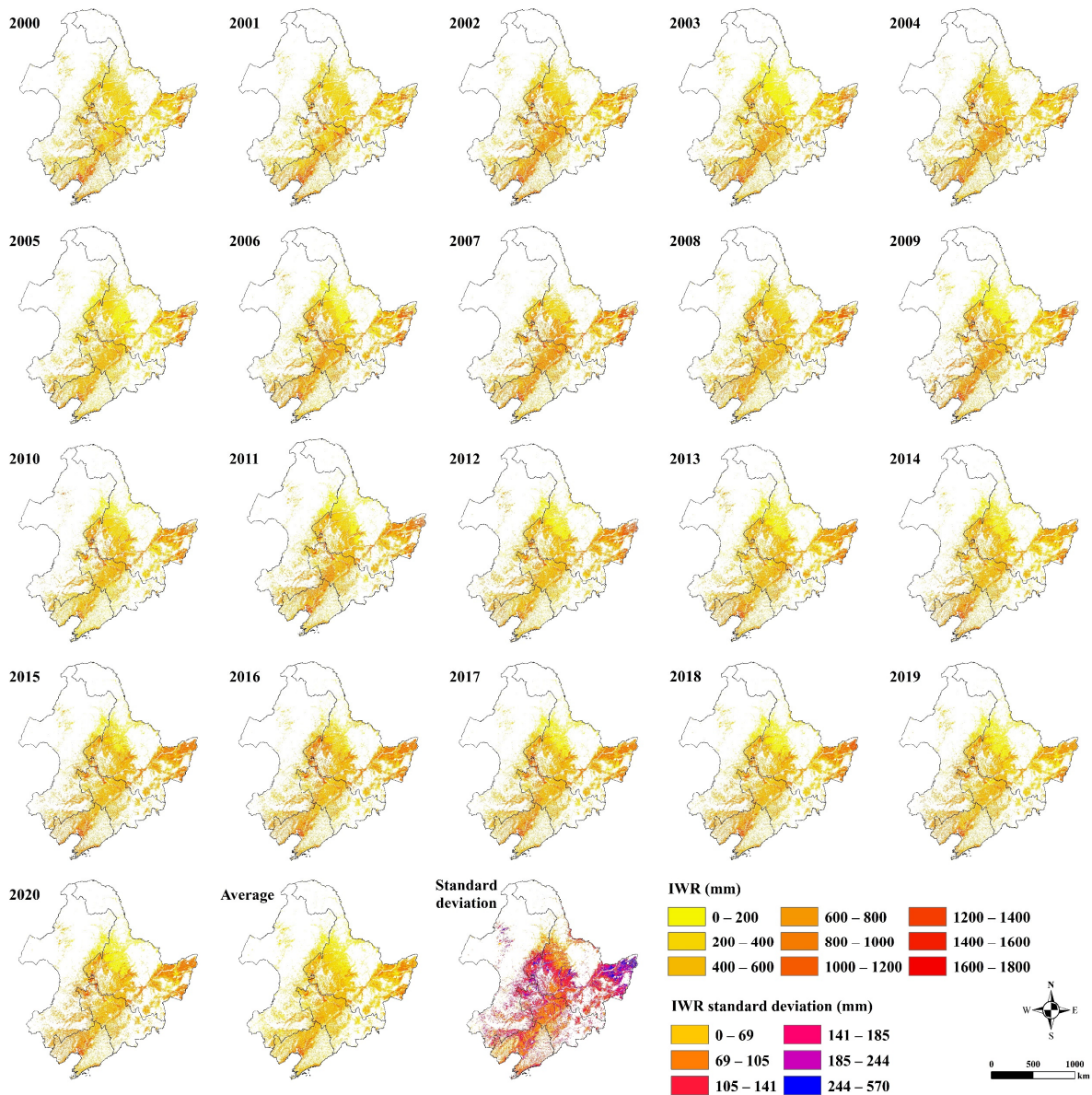


Figure 7. The spatial distribution of annual IWR and their average and standard deviation in the NEC from 2000 to 2020.

4.4. Annual Spatial Distribution and Temporal Changes in *M*

The average *M* showed an increasing trend in the NEC from 2000 to 2020 (Figure 3). *M* reached the highest value of 0.39 in 2005, while it reached the lowest value of 0.23 in 2007. The slope of *M* was 0.003/a and the slope% was 0.83%/a (Table 4). The average *M* for maize, rice, and soybean showed an increasing trend from 2000 to 2020 (Figure 4d). The average *M* value for maize reached the highest value of 0.34 in 2005, while it reached the lowest value of 0.20 in 2001. The average *M* value for rice reached the highest value of 0.25 in 2019, while it reached the lowest value of 0.12 in 2007. The average *M* for soybean reached the highest value of 0.67 in 2013, while it reached the lowest value of 0.28 in 2007. The multi-year average *M* values for maize, rice, and soybean were 0.27, 0.16, and 0.48, respectively. The slope of *M* from 2000 to 2020 for maize, rice, and soybean was 0.004/a, 0.004/a, and 0.01/a, and the slope% was 1.48%/a, 2.67%/a, and 2.87%/a, respectively (Table 4).

The average of *M* for maize was the highest in Heilongjiang at 0.29 and the lowest in Inner Mongolia at 0.19 (Table 5). The average of *M* for rice was the highest in Heilongjiang

at 0.164 and the lowest in Inner Mongolia at 0.12. The average for soybean was the highest in Heilongjiang at 0.53 and the lowest in Liaoning at 0.37. The standard deviation of M for maize was the highest in Jilin at 0.102 and the lowest in Liaoning at 0.062. The standard deviation of M for rice was the highest in Heilongjiang at 0.085 and the lowest in Inner Mongolia at 0.043. The standard deviation of M for soybean was the highest in Jilin at 0.12 and the lowest in Liaoning at 0.03.

The M had different spatial changes in 2000–2020 in the NEC (Figure 8). The average M from south to north showed a gradual increasing trend in the whole NEC during the past two decades. The maximum standard deviation of M was mainly distributed in the northern area in Heilongjiang, and the minimum standard deviation of M was mainly distributed in the southwestern area in Liaoning. Inner Mongolia showed a decreasing trend from the southern to the northern area. Heilongjiang narrowed from the center to the surroundings, which showed a trend of being higher in the central area and lower in the surroundings. Jilin and Liaoning had basically the same trend, which showed a trend of being lower in the center and higher in the surrounding areas. The maximum value of M was mainly distributed in the central area of Heilongjiang and showed a gradually decreasing trend from the central area to the surroundings from 2000 to 2020. The minimum value of M was mainly distributed in the central and eastern areas of Heilongjiang.

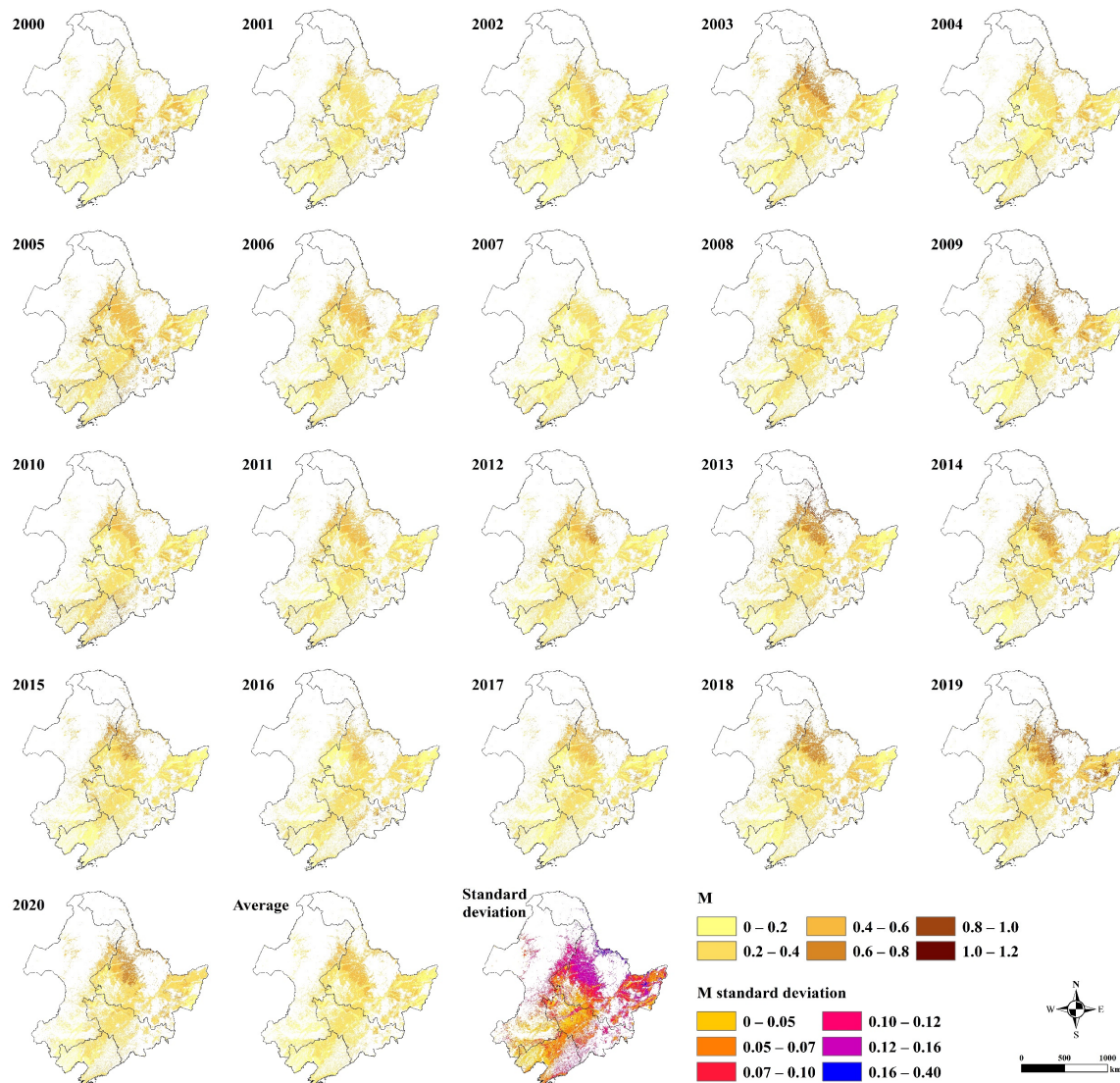


Figure 8. The spatial distribution of annual M and their average and standard deviation in the NEC from 2000 to 2020.

4.5. Impacts of Crop Type Change on IWR

The total IWR varied with crop area changes, which increased by $33.59 \times 10^9 \text{ m}^3$ (20.36%) in the NEC (Table 6). The total IWR of maize and rice showed an increasing trend, while the total IWR of soybean showed a decreasing trend from 2000 to 2020. The total IWR of maize and rice increased by $55.15 \times 10^9 \text{ m}^3$ (79.47%) and $32.83 \times 10^9 \text{ m}^3$ (109.18%), respectively, while the total IWR of soybean decreased by $54.39 \times 10^9 \text{ m}^3$ (−80.81%).

Table 6. Changes in the crop cultivation area and IWR in the NEC from 2000 to 2020.

Crop Type	Cultivation Area (10^6 ha)			IWR per Unit Area ($10^2 \text{ m}^3/\text{ha}$)			Total IWR (10^9 m^3)		
	2000	2020	Change	2000	2020	Change	2000	2020	Change
Maize	10.76	22.72	11.96	64.51	54.81	−9.69	69.40	124.55	55.15
Rice	2.71	6.73	4.02	111.07	93.47	−17.60	30.07	62.90	32.83
Soybean	21.46	7.71	−13.75	31.36	16.77	−14.59	67.31	12.92	−54.39

Crop type transfer has led to a change in irrigation water requirement, and this study analyzed two phases (Table 7). The transfer between different crop types resulted in an increase of $24.71 \times 10^9 \text{ m}^3$ in the total IWR in the NEC, which accounted for 39.28% of the total IWR change from 2000 to 2010. The expansion of the crop area resulted in an increase in the total IWR of $62.91 \times 10^9 \text{ m}^3$ (60.72%). The largest transfer from soybean to maize was $8.70 \times 10^6 \text{ ha}$; the total IWR increased by $17.57 \times 10^9 \text{ m}^3$ (27.93%). The transfers from maize and soybean to rice were $1.69 \times 10^6 \text{ ha}$ and $1.39 \times 10^6 \text{ ha}$, respectively. This resulted in the total IWR increasing by $4.78 \times 10^9 \text{ m}^3$ (7.60%) and $9.33 \times 10^9 \text{ m}^3$ (14.84%), respectively. However, the transfer from maize to soybean and the transfer from rice to maize and soybean resulted in reductions by $3.58 \times 10^9 \text{ m}^3$ (−5.69%), $2.83 \times 10^9 \text{ m}^3$ (−4.50%), and $0.56 \times 10^9 \text{ m}^3$ (−0.89%) in the total IWR, respectively.

Table 7. The contribution of crop type transfer rates to IWR in the NEC from 2000 to 2010.

Conversion Type	Converted Area (10^6 ha)	Contribution Value (10^9 m^3)	Contribution Rate (%)
Maize to Rice	1.69	4.78	7.60
Maize to Soybean	0.91	−3.58	−5.69
Rice to Maize	0.42	−2.83	−4.50
Rice to Soybean	0.06	−0.56	−0.89
Soybean to Maize	8.70	17.57	27.93
Soybean to Rice	1.39	9.33	14.84
Total	13.16	24.71	39.28

The transfer between different crop types resulted in an increase of $14.80 \times 10^9 \text{ m}^3$ in the total IWR in the NEC, which accounted for 41.25% of the total IWR change from 2010 to 2020 (Table 8). The largest transfer from soybean to maize was $4.16 \times 10^6 \text{ ha}$; the total IWR increased by $11.45 \times 10^9 \text{ m}^3$ (31.92%). The transfers from maize and soybean to rice were $1.11 \times 10^6 \text{ ha}$ and $0.50 \times 10^6 \text{ ha}$, respectively. This resulted in increases in the total IWR by $4.85 \times 10^9 \text{ m}^3$ (13.53%) and $3.43 \times 10^9 \text{ m}^3$ (9.57%), respectively. The transfer from maize to soybean and the transfer from rice to maize and soybean resulted in decreases by $2.01 \times 10^9 \text{ m}^3$ (−5.60%), $2.36 \times 10^9 \text{ m}^3$ (−6.58%), and $0.57 \times 10^9 \text{ m}^3$ (−1.59%) in the total IWR, respectively. The expansion of the crop area resulted in an increase in the total IWR of $35.87 \times 10^9 \text{ m}^3$ (58.75%).

Table 8. The contribution of crop type transfer rates to the IWR in the NEC from 2010 to 2020.

Conversion Type	Converted Area (10 ⁶ ha)	Contribution Value (10 ⁹ m ³)	Contribution Rate (%)
Maize to Rice	1.11	4.85	13.53
Maize to Soybean	0.72	−2.01	−5.60
Rice to Maize	0.69	−2.36	−6.58
Rice to Soybean	0.08	−0.57	−1.59
Soybean to Maize	4.16	11.45	31.92
Soybean to Rice	0.50	3.43	9.57
Total	7.27	14.80	41.25

4.6. Climate Impacts on Spatial Heterogeneity of ET_c and IWR

This study used gradient analysis to calculate the influences of key climate factors on ET_c and IWR. ET_c increased with increasing temperature in the NEC without distinguishing crops, and ET_c was reduced by temperature when the average temperature exceeded 5 °C (Figure 9). The effect of solar radiation on ET_c was similar to the effect of temperature on ET_c . However, the effect of precipitation on ET_c was to have basically no impact on ET_c as the precipitation increased. In terms of crop types, temperature had little effect on the ET_c for maize, while the ET_c increased with increasing temperature for rice and soybean. Precipitation for maize had little effect on ET_c , but the ET_c decreased with increasing precipitation for rice and soybean. The ET_c increased with increasing solar radiation for maize, rice, and soybean.

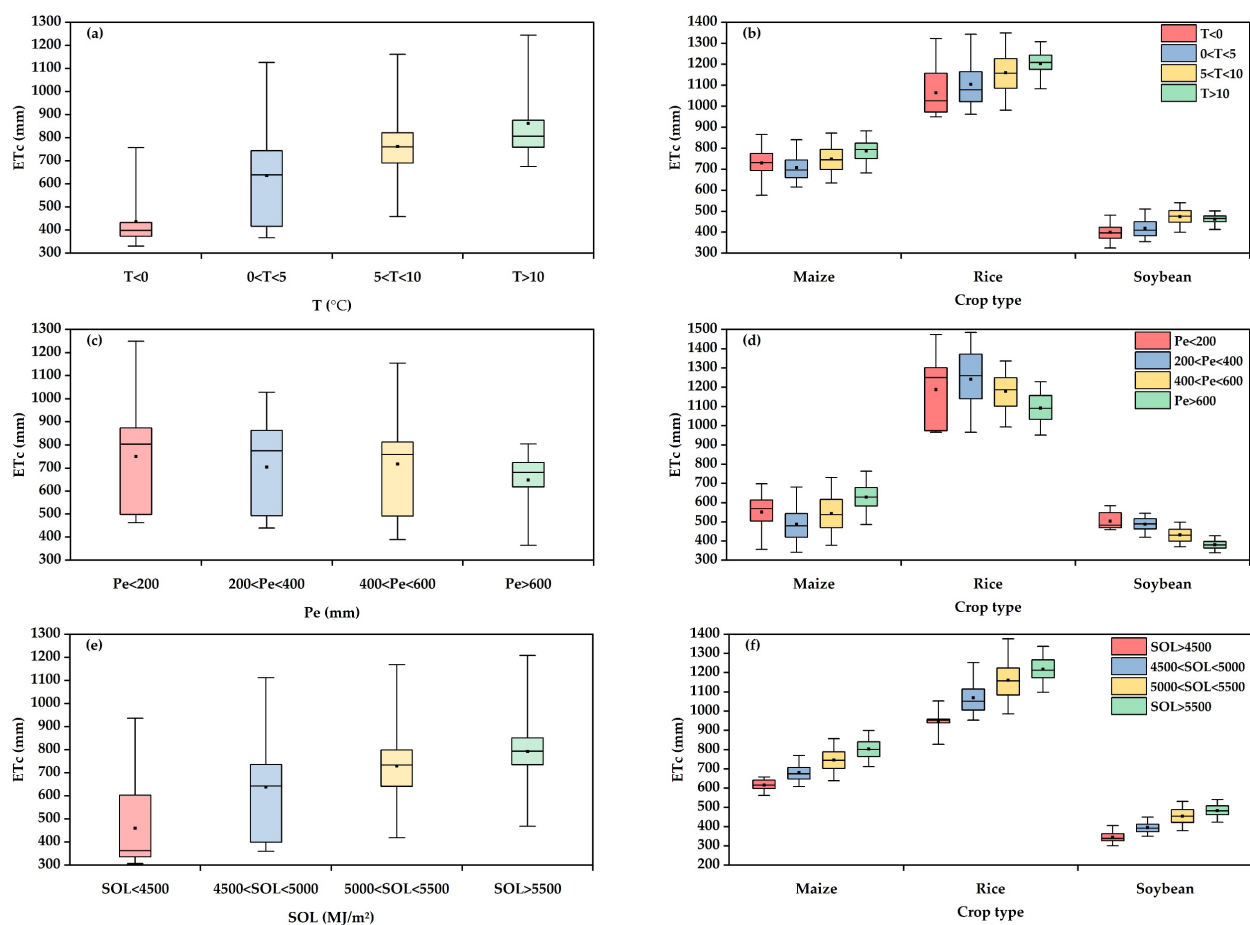


Figure 9. ET_c variations under different temperature gradients without distinguishing crops (a) and for different crops (b), under different precipitation gradients without distinguishing crops (c) and for different crops (d), and under different solar radiation gradients without distinguishing crops (e) and for different crops (f) in the NEC.

The IWR in the NEC increased with increasing temperature without distinguishing crops, and the IWR increased with increasing solar radiation (Figure 10). However, the IWR decreased with increasing precipitation. In terms of crop types, the temperature change for maize and rice had little effect on the IWR, but the IWR increased with the temperature increase in soybean. The IWR decreased with the increasing precipitation for maize, rice, and soybean. Solar radiation was the opposite to precipitation, and the IWR increased with increasing solar radiation for maize, rice, and soybean.

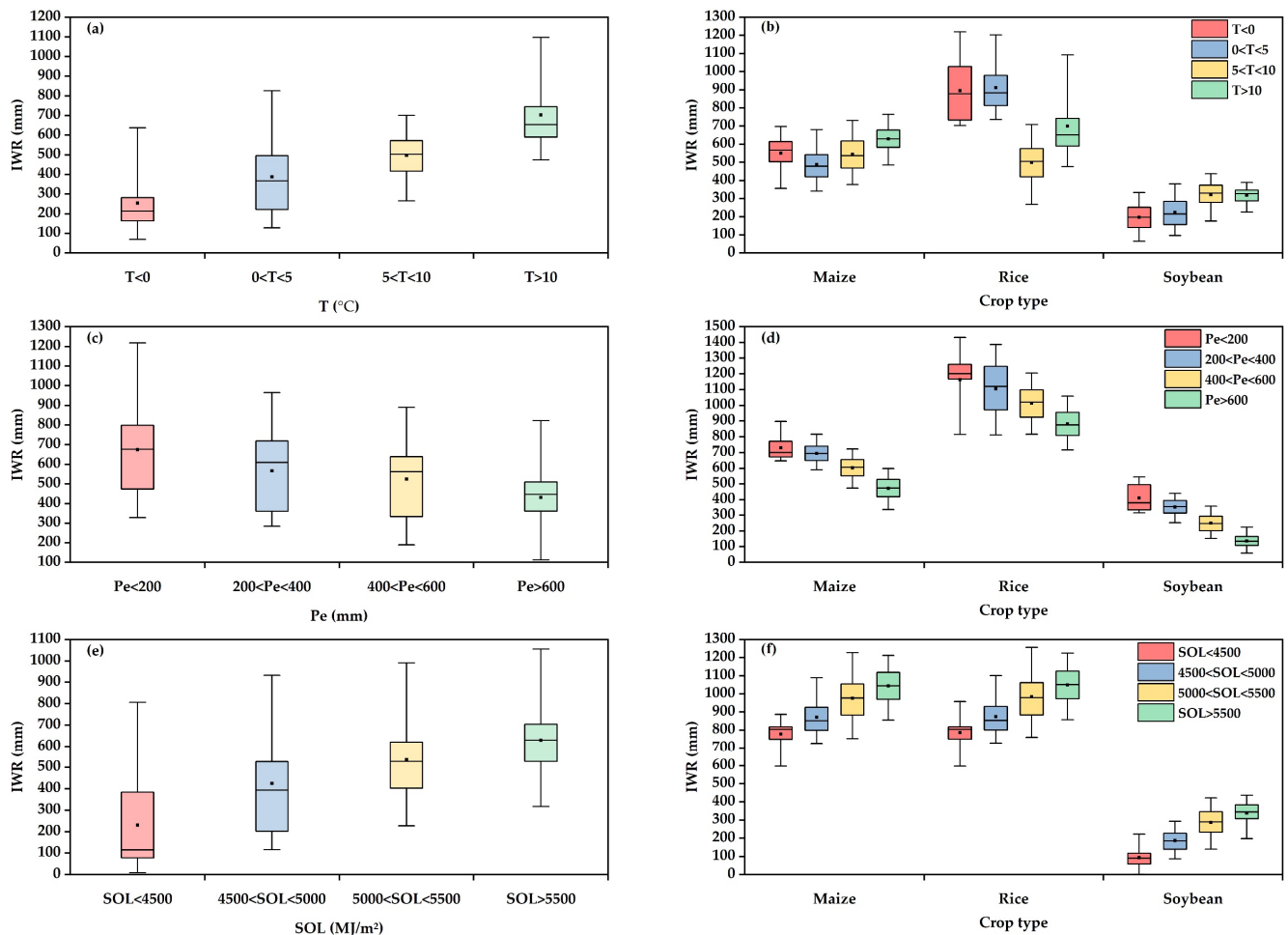


Figure 10. IWR variations under different temperature gradients without distinguishing crops (a) and for different crops (b), under different precipitation gradients without distinguishing crops (c) and for different crops (d), and under different solar radiation gradients without distinguishing crops (e) and for different crops (f) in the NEC.

5. Discussion

5.1. Reasons for the Spatiotemporal Heterogeneity of IWR

The increased irrigation water requirement is the main reason for changes in the crop planting structure, with the expansion of cultivated land having the greatest impact. Specifically, the expansion of maize and rice sowing amounted to 11.96×10^6 ha (111.15%) and 4.02×10^6 ha (148.34%), respectively, resulting in an increase in the total IWR by 55.15×10^9 m³ and 32.83×10^9 m³, respectively, which led to a water shortage of 87.98×10^9 m³. This is similar to Zhang's finding [46] that the expansion of water-intensive crops increases the amount of water used for agricultural irrigation and exacerbates the problem of water scarcity. Farmers tend to cultivate and increase the area of highly water-intensive maize and rice in order to increase their returns, which mainly because of the two crops have higher yields and economic benefits than soybean [37]. However, the

expansion has led to an increase in the agricultural water requirement, a decline in the groundwater levels, reduction in soil organic matter, and degradation of black soil, which is not conducive to sustainable agriculture development [57–61]. Thus, we should curb the massive expansion of water-intensive crops and encourage an increase in the area of soybean that is water-saving and soil-beneficial. In addition, we need to quantify the trade-offs and synergies of the multi-dimensional effects of different crop yields, agricultural water efficiency, and carbon sequestration when rationalizing the crop planting structure.

Climate change is another factor that generates heterogeneity in the irrigation water requirement. The results showed that the IWR was gradually decreased with increased precipitation for the three crops, but it was gradually increased with increased temperature and solar radiation for the three crops (Figure 10). Increased precipitation makes the land wetter, and the soil water storage function provides more adequate water during the critical growth period of crops, thus reducing the agricultural manual irrigation [62,63]. Increased temperature and solar radiation promoted the photosynthesis of crops, which led to increased evaporation and crops needing more water, thus leading to an increase in the irrigation water requirement [64–66].

In addition, the reasons affecting irrigation water requirement are not only the crop type and climate changes we analyzed, but also improvements in agricultural infrastructures and field management practices. The improvements in agricultural infrastructures included building high-standard farmland and improving the water and irrigation facilities. And field management practices include irrigation technology promotion and deep ploughing and tilling by large machinery that would enhance the soil water retention capacity.

5.2. Policy Recommendations and Practical Implications

Water resource consumption is extremely high, and agriculture uses the most water during irrigation, which leads to a decrease in water-use efficiency in the country [67,68]. Therefore, irrigation water saving and improving water resource utilization have become an important strategic task in maintaining sustainable socio-economic development [69,70]. There have been large-scale changes in crop type to increase economic and social incomes in the NEC. With the expansion of total crop cultivation, the crop cultivation area has far exceeded the maximum cultivation area that can be provided by the available water resources, which has ultimately led to an excess irrigation water requirement and severe water shortage [18,71]. Therefore, it is necessary to adjust the crop planting structure to reduce the cultivation of water-intensive crops and alleviate the imbalance in the agricultural water supply [72–74].

The IWR gradually increased from the northern to the southern area, and the IWR exceeded 1000 mm in severely water-scarce areas. The total crop irrigation water requirement far exceeded the maximum water supply in the NEC. This indicated that the effective precipitation has been unable to meet the amount of water required for crop growth in the NEC and needs agricultural irrigation measures [71,75]. Therefore, we propose to build water conservancy projects vigorously and set strict water quotas, strictly controlled crop water requirement in water-scarce areas, promote drip irrigation, sprinkler irrigation, rain harvesting and irrigation to achieve water-saving irrigation, and strengthen the precision management of the agricultural water requirement and reduce agricultural water losses [76–78].

5.3. Innovation, Deficiencies, and Prospects

Compared to previous studies [79–81], this study analyzed the annual spatiotemporal changes in the irrigation water requirement for different crops, calculated the amount of crop type transfer contributing to IWR, and explored the spatial heterogeneity of key climate factors on the ET_c and IWR. This study could provide some insight into the amount of water requirement for crop growth in different years and it improved the agricultural irrigation efficiency, and it was also possible to adjust the profitable crop cultivation to

agricultural producers and managers and provide recommendations for more effective water allocation.

However, this study only estimated the theoretical crop irrigation water requirement, not the actual irrigation water requirement. Future research could use multi-source remote-sensing data to reveal the spatial and temporal distribution for the actual crop irrigation water requirement and provide more comprehensive basic data for sustainable agricultural water management. In addition, the model parameters used in this study differed by crop type, but the parameters of the same crop in different spaces are the same. Future research could integrate RS vegetation indexes and technologies and field observations to map spatially-differentiated and crop-specific key parameters (e.g., growth period and K_c coefficients) for the more accurate estimation of agricultural water use in future studies. Moreover, we used gradient boxplots to analyze the impact of climate change on the ET_c and IWR, but we did not quantify the climatic contribution rate and the correlation coefficients between climatic factors and agricultural water use. Future research could use spatial correlation analysis and a structural equation model to analyze the correlation and quantitative contributions of key climate factors to agricultural water dynamics, supporting a more in-depth scientific basis for sustainable agricultural water management practices.

6. Conclusions

This study integrated multi-source data and multiple digital agriculture technologies to analyze annual crop-specific spatiotemporal changes in Pe , ET_c , IWR, and M , reveal the impacts of crop type and climate changes on agricultural water dynamics, and discuss the reasons and policy implications for spatiotemporally heterogeneous changes and impacts in the NEC from 2000 to 2020. The results indicated that regional average Pe , ET_c , IWR, and M increased by 1.56%/a, 0.74%/a, 0.42%/a, and 0.83%/a, respectively. Jointly influenced by crop type and climate changes, the regional total IWR increased from $166.78 \times 10^9 \text{ m}^3$ in 2000 to $200.37 \times 10^9 \text{ m}^3$ in 2020, of which 39.28% and 41.25% were attributed to crop type transfer, and the remaining 60.72% and 58.75% were caused by cropland expansion from 2000 to 2010 and 2010 to 2020, respectively. This suggested that we should curb the massive expansion of cropland and water-intensive crops and encourage the cultivation of water-saving and soil-beneficial soybean to reduce the IWR and promote agricultural sustainability. Gradient boxplot analysis found that the ET_c and IWR increased with increasing temperature and solar radiation, and increasing precipitation led to decreasing IWR in the NEC. The scientific implementation of crop planting structure adjustment and water-efficient management practices need to comprehensively quantify the trade-offs and synergies of the spatiotemporally heterogeneous multi-dimensional impacts of crop type and climate changes on agricultural water use and its efficiency, crop yield, and photosynthetic and soil carbon sequestration. Future studies could more accurately estimate agricultural water use through RS-based mapping of spatially differentiated parameters, and more synthetically quantify the impact mechanisms of key natural–anthropogenic factors to support the scientific basis for integrated water resource management and sustainable agricultural development.

Author Contributions: Conceptualization, X.X. and Y.L.; methodology, Y.L.; software, J.Z.; validation, X.X., J.Z. and Y.L.; formal analysis, Y.L.; data curation, J.Z.; writing—original draft preparation, X.X., J.Z. and Y.L.; writing—review and editing, Y.L.; visualization, J.Z.; supervision, Y.L.; project administration, X.X. and Y.L.; funding acquisition, Y.L. All authors have read and agreed to the published version of the manuscript.

Funding: This research was funded by National Natural Science Foundation of China (Grant Nos. 42201289 and 42293270), the National Key Research and Development Program of China (Grant No. 2023YFD1501001), the Natural Science Foundation of Shandong Province (Grant No. ZR2023MD018), the China Postdoctoral Science Foundation (Grant No. 2021M700143), and the Strategic Priority Research Program of the Chinese Academy of Sciences (Grant No. XDA28130400).

Data Availability Statement: The data presented in this research are available on reasonable request from the corresponding author. The data are not publicly available due to the data need to be used for further research.

Acknowledgments: We greatly appreciate the editors and anonymous reviewers for their valuable time, constructive suggestions, and insightful comments.

Conflicts of Interest: The authors declare no conflicts of interest.

References

- Field, C.B.; Michalak, A.M. Water, Climate, Energy, Food: Inseparable & Indispensable. *Daedalus* **2015**, *144*, 7–17. [[CrossRef](#)]
- Eliasson, J. The Rising Pressure of Global Water Shortages. *Nature* **2015**, *517*, 6. [[CrossRef](#)]
- Rosa, L.; Chiarelli, D.D.; Rulli, M.C.; Dell’Angelo, J.; D’Odorico, P. Global Agricultural Economic Water Scarcity. *Sci. Adv.* **2020**, *6*, eaaz6031. [[CrossRef](#)]
- Schultz, B.; Thatte, C.; Labhsetwar, V. Irrigation and Drainage. Main Contributors to Global Food Production. *Irrig. Drain.* **2005**, *54*, 263–278. [[CrossRef](#)]
- Calzadilla, A.; Rehdanz, K.; Betts, R.; Falloon, P.; Wiltshire, A.; Tol, R.S. Climate Change Impacts on Global Agriculture. *Clim. Chang.* **2013**, *120*, 357–374. [[CrossRef](#)]
- Guo, B.; Li, W.; Guo, J.; Chen, C. Risk Assessment of Regional Irrigation Water Demand and Supply in an Arid Inland River Basin of Northwestern China. *Sustainability* **2015**, *7*, 12958–12973. [[CrossRef](#)]
- Song, W.; Pijanowski, B.C.; Tayyebi, A. Urban Expansion and Its Consumption of High-Quality Farmland in Beijing, China. *Ecol. Indic.* **2015**, *54*, 60–70. [[CrossRef](#)]
- Caldera, U.; Breyer, C. Strengthening the Global Water Supply through a Decarbonised Global Desalination Sector and Improved Irrigation Systems. *Energy* **2020**, *200*, 117507. [[CrossRef](#)]
- Han, S.; Tian, F.; Gao, L. Current Status and Recent Trend of Irrigation Water Use in China. *Irrig. Drain.* **2020**, *69*, 25–35. [[CrossRef](#)]
- Calow, R.C.; Howarth, S.E.; Wang, J. Irrigation Development and Water Rights Reform in China. *Int. J. Water Resour. Dev.* **2009**, *25*, 227–248. [[CrossRef](#)]
- McLaughlin, D.; Kinzelbach, W. Food Security and Sustainable Resource Management. *Water Resour. Res.* **2015**, *51*, 4966–4985. [[CrossRef](#)]
- Li, H.; Du, X.; Lu, X.; Fang, M. Analysis of Groundwater Overexploitation Based on Groundwater Regime Information. *Groundwater* **2023**, *61*, 692–705. [[CrossRef](#)]
- Shen, H.; Leblanc, M.; Tweed, S.; Liu, W. Groundwater Depletion in the Hai River Basin, China, from in Situ and Grace Observations. *Hydrol. Sci. J.* **2015**, *60*, 671–687. [[CrossRef](#)]
- Howell, T.A. Enhancing Water Use Efficiency in Irrigated Agriculture. *Agron. J.* **2001**, *93*, 281–289. [[CrossRef](#)]
- Kadiresan, K.; Khanal, P.R. Rethinking Irrigation for Global Food Security. *Irrig. Drain.* **2018**, *67*, 8–11. [[CrossRef](#)]
- Li, X.; Jiang, W.; Duan, D. Spatio-Temporal Analysis of Irrigation Water Use Coefficients in China. *J. Environ. Manag.* **2020**, *262*, 110242. [[CrossRef](#)]
- Xiong, W.; Holman, I.; Lin, E.; Conway, D.; Jiang, J.; Xu, Y.; Li, Y. Climate Change, Water Availability and Future Cereal Production in China. *Agric. Ecosyst. Environ.* **2010**, *135*, 58–69. [[CrossRef](#)]
- Cai, X.; McKinney, D.C.; Rosegrant, M.W. Sustainability Analysis for Irrigation Water Management in the Aral Sea Region. *Agric. Syst.* **2003**, *76*, 1043–1066. [[CrossRef](#)]
- Sun, H.; Shen, Y.; Yu, Q.; Flerchinger, G.N.; Zhang, Y.; Liu, C.; Zhang, X. Effect of Precipitation Change on Water Balance and Wue of the Winter Wheat–Summer Maize Rotation in the North China Plain. *Agric. Water Manag.* **2010**, *97*, 1139–1145. [[CrossRef](#)]
- Bhat, O.A.; Lone, M.A.; Kumar, R. Determination of Water Requirement and Crop Coefficients for Green Gram in Temperate Region Using Lysimeter Water Balance. *Int. J. Hydrol. Sci. Technol.* **2021**, *12*, 1–15. [[CrossRef](#)]
- Kadam, S.; Gorantiwar, S.; Mandre, N.; Tale, D. Crop Coefficient for Potato Crop Evapotranspiration Estimation by Field Water Balance Method in Semi-Arid Region, Maharashtra, India. *Potato. Res.* **2021**, *64*, 421–433. [[CrossRef](#)]
- Ray, S.; Dadhwal, V. Estimation of Crop Evapotranspiration of Irrigation Command Area Using Remote Sensing and Gis. *Agric. Water Manag.* **2001**, *49*, 239–249. [[CrossRef](#)]
- Liu, Y.; Song, W.; Deng, X. Spatiotemporal Patterns of Crop Irrigation Water Requirements in the Heihe River Basin, China. *Water* **2017**, *9*, 616. [[CrossRef](#)]
- Mujere, N. Assessing Risks and Resilience to Hydro-Meteorological Disasters. In *Disaster Risk Reduction for Resilience: Climate Change and Disaster Risk Adaptation*; Springer International Publishing: Cham, Switzerland, 2023; pp. 143–159.
- Abedinpour, M.; Sarangi, A.; Rajput, T.; Singh, M.; Pathak, H.; Ahmad, T. Performance Evaluation of Aquacrop Model for Maize Crop in a Semi-Arid Environment. *Agric. Water Manag.* **2012**, *110*, 55–66. [[CrossRef](#)]
- Bocchiola, D. Impact of Potential Climate Change on Crop Yield and Water Footprint of Rice in the Po Valley of Italy. *Agric. Syst.* **2015**, *139*, 223–237. [[CrossRef](#)]
- Pasquel, D.; Roux, S.; Richetti, J.; Cammarano, D.; Tisseyre, B.; Taylor, J.A. A Review of Methods to Evaluate Crop Model Performance at Multiple and Changing Spatial Scales. *Precis. Agric.* **2022**, *23*, 1489–1513. [[CrossRef](#)]

28. Zhou, K.; Wang, Y.; Chang, J.; Zhou, S.; Guo, A. Spatial and Temporal Evolution of Drought Characteristics across the Yellow River Basin. *Ecol. Indic.* **2021**, *131*, 108207. [[CrossRef](#)]
29. Cobaner, M. Evapotranspiration Estimation by Two Different Neuro-Fuzzy Inference Systems. *J. Hydrol.* **2011**, *398*, 292–302. [[CrossRef](#)]
30. Lang, D.; Zheng, J.; Shi, J.; Liao, F.; Ma, X.; Wang, W.; Chen, X.; Zhang, M. A Comparative Study of Potential Evapotranspiration Estimation by Eight Methods with Fao Penman–Monteith Method in Southwestern China. *Water* **2017**, *9*, 734. [[CrossRef](#)]
31. Nana, E.; Corbari, C.; Bocchiola, D. A Model for Crop Yield and Water Footprint Assessment: Study of Maize in the Po Valley. *Agric. Syst.* **2014**, *127*, 139–149. [[CrossRef](#)]
32. Solangi, G.S.; Shah, S.A.; Alharbi, R.S.; Panhwar, S.; Keerio, H.A.; Kim, T.-W.; Memon, J.A.; Bughio, A.D. Investigation of Irrigation Water Requirements for Major Crops Using Cropwat Model Based on Climate Data. *Water* **2022**, *14*, 2578. [[CrossRef](#)]
33. Rossi, R.E.; Mulla, D.J.; Journel, A.G.; Franz, E.H. Geostatistical Tools for Modeling and Interpreting Ecological Spatial Dependence. *Ecol. Monogr.* **1992**, *62*, 277–314. [[CrossRef](#)]
34. House-Peters, L.A.; Chang, H. Urban Water Demand Modeling: Review of Concepts, Methods, and Organizing Principles. *Water Resour. Res.* **2011**, *47*, W05401. [[CrossRef](#)]
35. He, B.; Lü, A.; Wu, J.; Zhao, L.; Liu, M. Drought Hazard Assessment and Spatial Characteristics Analysis in China. *J. Geogr. Sci.* **2011**, *21*, 235–249. [[CrossRef](#)]
36. Yu, X.; He, X.; Zheng, H.; Guo, R.; Ren, Z.; Zhang, D.; Lin, J. Spatial and Temporal Analysis of Drought Risk During the Crop-Growing Season over Northeast China. *Nat. Hazards* **2014**, *71*, 275–289. [[CrossRef](#)]
37. Liu, Y.; Wang, J. Revealing Annual Crop Type Distribution and Spatiotemporal Changes in Northeast China Based on Google Earth Engine. *Remote Sens.* **2022**, *14*, 4056. [[CrossRef](#)]
38. Zhang, L.; Chen, F.; Lei, Y. Climate Change and Shifts in Cropping Systems Together Exacerbate China’s Water Scarcity. *Environ. Res. Lett.* **2020**, *15*, 104060. [[CrossRef](#)]
39. Huai, H.; Chen, X.; Huang, J.; Chen, F. Water-Scarcity Footprint Associated with Crop Expansion in Northeast China: A Case Study Based on Aquacrop Modeling. *Water* **2019**, *12*, 125. [[CrossRef](#)]
40. Yang, X.; Jin, X.; Chu, Q.; Pacenka, S.; Steenhuis, T.S. Impact of Climate Variation from 1965 to 2016 on Cotton Water Requirements in North China Plain. *Agric. Water Manag.* **2021**, *243*, 106502. [[CrossRef](#)]
41. Wang, J.; Xin, L.; Wang, X.; Jiang, M. The Impact of Climate Change and Grain Planting Structure Change on Irrigation Water Requirement for Main Grain Crops in Mainland China. *Land* **2022**, *11*, 2174. [[CrossRef](#)]
42. Zhang, J.; Deng, M.; Han, Y.; Huang, H.; Yang, T. Spatiotemporal Variation of Irrigation Water Requirements for Grain Crops under Climate Change in Northwest China. *Environ. Sci. Pollut. Res.* **2023**, *30*, 45711–45724. [[CrossRef](#)]
43. Xu, H.; Tian, Z.; He, X.; Wang, J.; Sun, L.; Fischer, G.; Fan, D.; Zhong, H.; Wu, W.; Pope, E. Future Increases in Irrigation Water Requirement Challenge the Water-Food Nexus in the Northeast Farming Region of China. *Agric. Water Manag.* **2019**, *213*, 594–604. [[CrossRef](#)]
44. Lai, J.; Li, Y.; Chen, J.; Niu, G.-Y.; Lin, P.; Li, Q.; Wang, L.; Han, J.; Luo, Z.; Sun, Y. Massive Crop Expansion Threatens Agriculture and Water Sustainability in Northwestern China. *Environ. Res. Lett.* **2022**, *17*, 034003. [[CrossRef](#)]
45. Luo, W.; Chen, M.; Kang, Y.; Li, W.; Li, D.; Cui, Y.; Khan, S.; Luo, Y. Analysis of Crop Water Requirements and Irrigation Demands for Rice: Implications for Increasing Effective Rainfall. *Agric. Water Manag.* **2022**, *260*, 107285. [[CrossRef](#)]
46. Zhang, Q.; Sun, J.; Zhang, G.; Liu, X.; Wu, Y.; Sun, J.; Hu, B. Spatiotemporal Dynamics of Water Supply–Demand Patterns under Large-Scale Paddy Expansion: Implications for Regional Sustainable Water Resource Management. *Agric. Water Manag.* **2023**, *285*, 108388. [[CrossRef](#)]
47. Chi, D.; Wang, H.; Li, X.; Liu, H.; Li, X. Estimation of the Ecological Water Requirement for Natural Vegetation in the Ergune River Basin in Northeastern China from 2001 to 2014. *Ecol. Indic.* **2018**, *92*, 141–150. [[CrossRef](#)]
48. Wang, T.; Du, C.; Nie, T.; Sun, Z.; Zhu, S.; Feng, C.; Dai, C.; Chu, L.; Liu, Y.; Liang, Q. Spatiotemporal Analysis of Maize Water Requirement in the Heilongjiang Province of China During 1960–2015. *Water* **2020**, *12*, 2472. [[CrossRef](#)]
49. Ren, Z.; Liu, X. Temporal and Spatial Trends of Spring Maize Irrigation Water Requirement in Northeast China in Recent 60 Years. In Proceedings of the Sixth Symposium of Risk Analysis and Risk Management in Western China (WRARM 2019), Kunming, China, 16–17 November 2019; pp. 28–32.
50. Hutchinson, M.F.; Xu, T. *Anusplin Version 4.2 User Guide*; Centre for Resource and Environmental Studies, The Australian National University: Canberra, Australia, 2004; Volume 54.
51. Döll, P.; Siebert, S. Global Modeling of Irrigation Water Requirements. *Water Resour. Res.* **2002**, *38*, 8-1–8-10. [[CrossRef](#)]
52. Geng, Q.; Zhao, Y.; Sun, S.; He, X.; Wang, D.; Wu, D.; Tian, Z. Spatio-Temporal Changes and Its Driving Forces of Irrigation Water Requirements for Cotton in Xinjiang, China. *Agric. Water Manag.* **2023**, *280*, 108218. [[CrossRef](#)]
53. Jia, K.; Yang, Y.; Dong, G.; Zhang, C.; Lang, T. Variation and Determining Factor of Winter Wheat Water Requirements under Climate Change. *Agric. Water Manag.* **2021**, *254*, 106967. [[CrossRef](#)]
54. Allen, R.G.; Pereira, L.S.; Raes, D.; Smith, M. *Crop Evapotranspiration-Guidelines for Computing Crop Water Requirements-Fao Irrigation and Drainage Paper 56*; Food and Agriculture Organization: Rome, Italy, 1998; Volume 300, p. D05109.
55. Ren, X.L.; Li, H.L.; Zhang, Y.H.; Pu, X.; Zhang, L.L. Water Requirement Characteristics and Influencing Factors of Main Crops in the Sanjiang Plain from 2000 to 2015. *Arid Land Geogr.* **2019**, *42*, 854–866. (In Chinese) [[CrossRef](#)]

56. Smith, M. *Cropwat: A Computer Program for Irrigation Planning and Management*; Food & Agriculture Organization: Rome, Italy, 1992.
57. Cates, A.M.; Ruark, M.D.; Hedtcke, J.L.; Posner, J.L. Long-Term Tillage, Rotation and Perennialization Effects on Particulate and Aggregate Soil Organic Matter. *Soil. Tillage Res.* **2016**, *155*, 371–380. [[CrossRef](#)]
58. Hu, X.; Chen, M.; Liu, D.; Li, D.; Jin, L.; Liu, S.; Cui, Y.; Dong, B.; Khan, S.; Luo, Y. Reference Evapotranspiration Change in Heilongjiang Province, China from 1951 to 2018: The Role of Climate Change and Rice Area Expansion. *Agric. Water Manag.* **2021**, *253*, 106912. [[CrossRef](#)]
59. Singh, K.; Sidhpuria, M.; Jhorar, R.; Kumar, A.; Singh, J.; Mehla, M.K. Energy Utilization for Ground Water Pumping under Declining Water Table Scenario: A Review. *Int. J. Econ. Plants* **2021**, *8*, 136–142. [[CrossRef](#)]
60. Tang, Q.; Hua, L.; Cao, Y.; Jiang, L.; Cai, C. Human Activities Are the Key Driver of Water Erosion Changes in Northeastern China. *Land. Degrad. Dev.* **2024**, *35*, 62–75. [[CrossRef](#)]
61. Yang, L.; Yang, Y.; Feng, Z.; Zheng, Y. Effect of Maize Sowing Area Changes on Agricultural Water Consumption from 2000 to 2010 in the West Liaohe Plain, China. *J. Integr. Agric.* **2016**, *15*, 1407–1416. [[CrossRef](#)]
62. Thomas, A. Agricultural Irrigation Demand under Present and Future Climate Scenarios in China. *Glob. Planet. Chang.* **2008**, *60*, 306–326. [[CrossRef](#)]
63. Yosef, B.A.; Asmamaw, D.K. Rainwater Harvesting: An Option for Dry Land Agriculture in Arid and Semi-Arid Ethiopia. *Int. J. Water Resour. Environ. Eng.* **2015**, *7*, 17–28. [[CrossRef](#)]
64. Cascone, S.; Coma, J.; Gagliano, A.; Pérez, G. The Evapotranspiration Process in Green Roofs: A Review. *Build. Environ.* **2019**, *147*, 337–355. [[CrossRef](#)]
65. Mo, X.; Chen, X.; Hu, S.; Liu, S.; Xia, J. Attributing Regional Trends of Evapotranspiration and Gross Primary Productivity with Remote Sensing: A Case Study in the North China Plain. *Hydrol. Earth. Syst. Sci.* **2017**, *21*, 295–310. [[CrossRef](#)]
66. Boonwichai, S.; Shrestha, S.; Babel, M.S.; Weesakul, S.; Datta, A. Climate Change Impacts on Irrigation Water Requirement, Crop Water Productivity and Rice Yield in the Songkhram River Basin, Thailand. *J. Clean. Prod.* **2018**, *198*, 1157–1164. [[CrossRef](#)]
67. Hongyun, H.; Liange, Z. Chinese Agricultural Water Resource Utilization: Problems and Challenges. *Water Policy* **2007**, *9*, 11–28. [[CrossRef](#)]
68. Ju, Q.; Du, L.; Liu, C.; Jiang, S. Water Resource Management for Irrigated Agriculture in China: Problems and Prospects. *Irrig. Drain.* **2023**, *72*, 854–863. [[CrossRef](#)]
69. Li, M.; Cao, X.; Liu, D.; Fu, Q.; Li, T.; Shang, R. Sustainable Management of Agricultural Water and Land Resources under Changing Climate and Socio-Economic Conditions: A Multi-Dimensional Optimization Approach. *Agric. Water Manag.* **2022**, *259*, 107235. [[CrossRef](#)]
70. Wang, S.; Wei, Y. Water Resource System Risk and Adaptive Management of the Chinese Heihe River Basin in Asian Arid Areas. *Mitig. Adapt. Strateg. Glob. Chang.* **2019**, *24*, 1271–1292. [[CrossRef](#)]
71. Zhang, L.; Cong, Z.; Zhang, D.; Li, Q. Response of Vegetation Dynamics to Climatic Variables across a Precipitation Gradient in the Northeast China Transect. *Hydrol. Sci. J.* **2017**, *62*, 1517–1531. [[CrossRef](#)]
72. Liu, J.; Sun, B.; Shen, H.; Ding, P.; Ning, D.; Zhang, J.; Qiu, X. Crop Water Requirement and Utilization Efficiency-Based Planting Structure Optimization in the Southern Huang-Huai-Hai Plain. *Agronomy* **2022**, *12*, 2219. [[CrossRef](#)]
73. Ren, D.; Yang, Y.; Yang, Y.; Richards, K.; Zhou, X. Land-Water-Food Nexus and Indications of Crop Adjustment for Water Shortage Solution. *Sci. Total Environ.* **2018**, *626*, 11–21. [[CrossRef](#)]
74. Yang, G.; Li, S.; Wang, H.; Wang, L. Study on Agricultural Cultivation Development Layout Based on the Matching Characteristic of Water and Land Resources in North China Plain. *Agric. Water Manag.* **2022**, *259*, 107272. [[CrossRef](#)]
75. Liu, Z.; Yang, X.; Lin, X.; Gowda, P.; Lv, S.; Wang, J. Climate Zones Determine Where Substantial Increases of Maize Yields Can Be Attained in Northeast China. *Clim. Chang.* **2018**, *149*, 473–487. [[CrossRef](#)]
76. Deng, X.-P.; Shan, L.; Zhang, H.; Turner, N.C. Improving Agricultural Water Use Efficiency in Arid and Semiarid Areas of China. *Agric. Water Manag.* **2006**, *80*, 23–40. [[CrossRef](#)]
77. Yang, X.; Pu, Y.; Weng, S.; Hou, M.; Wang, Z. Review of Agricultural Water-Saving Policies and Measures in Recent Years—a Case Study of Jiangsu Province, China. *Water Supply* **2022**, *22*, 3951–3967. [[CrossRef](#)]
78. Zhang, W.; Sheng, J.; Li, Z.; Weindorf, D.C.; Hu, G.; Xuan, J.; Zhao, H. Integrating Rainwater Harvesting and Drip Irrigation for Water Use Efficiency Improvements in Apple Orchards of Northwest China. *Sci. Hortic.* **2021**, *275*, 109728. [[CrossRef](#)]
79. Lei, H.; Qiao, S.; Pan, H.; Shang, C. Temporal and Spatial Distribution of Agricultural Irrigation Water Requirement and Irrigation Requirement Index in Guizhou Province. *Trans. CSAE* **2016**, *32*, 115–121. [[CrossRef](#)]
80. Nie, T.; Liang, Q.; Wang, T.; Chu, L.; Chen, X.; Li, F. Water Requirement and Supply and Irrigation Schedule Formulation for Maize in the Western Region of Heilongjiang Province. *South-North Water Transf. Water Sci. Technol.* **2021**, *19*, 960–971. [[CrossRef](#)]
81. Xu, C.; Lu, C.; Sun, Q. Impact of Climate Change on Irrigation Water Requirement of Wheat Growth—A Case Study of the Beijing-Tianjin-Hebei Region in China. *Urban Clim.* **2021**, *39*, 100971. [[CrossRef](#)]

Disclaimer/Publisher’s Note: The statements, opinions and data contained in all publications are solely those of the individual author(s) and contributor(s) and not of MDPI and/or the editor(s). MDPI and/or the editor(s) disclaim responsibility for any injury to people or property resulting from any ideas, methods, instructions or products referred to in the content.